

BUCKLING OF ISOTROPIC AND ORTHOTROPIC
WEBS

By

VINDHYA NUKALA

Bachelor of Technology in Mechanical Engineering

Jawaharlal Nehru Technological University

Hyderabad, Telangana.

2013

Submitted to the Faculty of the
Graduate College of the
Oklahoma State University
in partial fulfillment of
the requirements for
the Degree of
MASTER OF SCIENCE
July, 2016

BUCKLING OF ISOTROPIC AND ORTHOTROPIC
WEBS

Thesis Approved:

Dr. James K. Good

Thesis Adviser

Dr. Delahoussaye

Dr. Wang

ACKNOWLEDGEMENTS

I would like to convey my sincere gratitude to my graduate advisor Dr. James K. Good for his immense support and exceptional guidance throughout my research. He has been extremely helpful in clarifying all questions and steered me out of the problems during the research. This research would have been not possible without him.

I would like to extend my sincere thanks to my committee members, Dr. Wang and Dr. Delahoussaye for offering valuable suggestions. I am very grateful to Mr. Ron Markum for his indispensable support in every step to conduct the experiments in an accurate and timely manner. Special thanks to the WHRC sponsors for funding this project. I would like to thank my fellow graduate research students for their encouragement and support to accomplish this project.

I would like to offer my special thanks to my parents Ravinder Reddy Nukala, Suvarna Nukala and my elder brother Phaninder Nukala for their never-ending love and support.

Name: VINDHYA NUKALA

Date of Degree: JULY, 2016

Title of Study: BUCKLING OF ISOTROPIC AND ORTHOTROPIC WEBS

Major Field: MECHANICAL AND AEROSPACE ENGINEERING

Abstract:

A web is a material that is very long compared to its width. Webs are usually quite thin compared to their width dimension and are stored and transported in the form of rolls. Webs are often subjected to several continuous processes in which value is added prior to manufacturing a final product. During these processes the web is first unwound and then transported over a series of rollers, some of which are driven and others not, through the process and then finally rewound to await the next process. The direction in which web is travelled is called as the machine direction and the direction orthogonal to machine direction but still within the plane of the web is called as the cross machine direction. The objective is to transport these webs through processes with minimal defects and economic loss. Due to the small thickness of the web, the bending stiffness of the web is also small, and web tension is often sufficient to take the shape of the roller surface as the web transmits the roller. The unsupported web between rollers is called a free span and in good processing conditions, this web has the form of a flat plate in free span. Often web instability can be witnessed in free span called web troughs.

The web troughs form because of compressive stresses in cross machine direction. Good and Beisel has estimated the critical compressive required to induce troughs and estimated the wavelength of troughs in webs. Cerda et al developed an inextensibility theory to predict the amplitude of troughs in isotropic webs. A closed form expression to predict the troughs amplitude and wavelength could be very useful. Most of the webs have orthotropic material properties. This research is to extend the inextensibility theory to orthotropic webs and to verify the theory of elastic isotropic and orthotropic web materials. The validity of the troughs amplitude and wavelength expressions will be achieved through laboratory tests and nonlinear finite element simulations. Furthermore, limitations of these expressions will be studied.

TABLE OF CONTENTS

Chapter	Page
I. INTRODUCTION.....	1
An Introduction to Webs.....	1
Web Instability.....	2
The Theory of Inextensibility.....	4
This Research.....	4
II. LITERATURE SURVEY.....	5
Wavelength of Troughs on Isotropic webs.....	5
Wavelength of Troughs on Orthotropic webs.....	9
Amplitude of Troughs on Isotropic Webs.....	11
Research Objective.....	18
III. AMPLITUDE OF TROUGHS ON ORTHOTROPIC WEBS.....	19
Expression for Amplitude of Troughs on Orthotropic Webs.....	19
IV. EXPERIMENTAL SETUP AND MATERIAL PROPERTIES.....	21
Experimental Setup to Analyze the Profile of Troughs.....	23
Preparation of Specimens.....	26
Measurement of Material Properties.....	27
V. FINITE ELEMENT MODEL.....	34
Finite Element Analysis Using Abaqus 6.14.....	34
VI. RESULTS AND COMPARISONS.....	38
Experimental and Abaqus Results of Isotropic Web.....	38

Chapter	Page
Comparison with Theoretical Results of Isotropic web.....	46
Experimental and Abaqus Results of Orthotropic Web.....	49
Comparison with Theoretical Results of Orthotropic web	56
 VII. CONCLUSION AND FUTURE SYUDY	 63
Conclusions.....	63
Future Study.....	64
 REFERENCES	 66
 APPENDICES	 68

LIST OF TABLES

Table	Page
4-1 - Material Properties of Polyester Web	28
4-2 - Test data of Young's Modulus in MD	30
4-3 - Young's Modulus in MD of Four Different Tests	30
4-4 - Test Data of Young's Modulus in CMD.....	32
4-5 - Young's Modulus in CMD of Four Different Tests.....	33
4-6 - Material Properties of the Orthotropic Web.....	33
6-1 - Experimental Results of Wavelength on the Isotropic Web (in).....	42
6-2 - Experimental Results of Amplitude on the Isotropic Web (in).....	43
6-3 - Comparison of Wavelength with Theoretical Results on the Isotropic Web	46
6-4 - Comparison of Amplitude with Theoretical Results on the Isotropic web	47
6-5 - Experiment Results of Wavelength on the Orthotropic Web.....	52
6-6 - Experiment Results of Amplitude on the Orthotropic Web	53
6-7 - Comparison of Experiment and Theoretical Wavelength on the Orthotropic Web	56
6-8 - Comparison of Experiment and Theoretical Amplitude on the Orthotropic Web	57
6-9 - Material Properties of a Pseudo Material	58
6-10 - Comparison of Abaqus and Theoretical Wavelength on the Orthotropic Web.....	61
6-11 - Comparison of Abaqus and Theoretical Amplitude on the Orthotropic Web.....	62

LIST OF FIGURES

Figure	Page
1-1 - A Web Travelling Through a Process Machine.....	1
1-2 - Web Trough Instability	2
1-3 - Web Wrinkles on Rollers.....	3
2-1 - Rectangular Plate under Biaxial Stress with Simply Support Edges	5
2-2 - Wrinkles on Polyethylene Sheet	16
4-1 - CMD Stresses in a Polyester Web	22
4-2 - CMD Stresses in a Polyester Web (Refined Scale)	22
4-3 - Experimental Setup.....	24
4-4 - LabView Program.....	25
4-5 - The Splice Table	26
4-6 - Splice Table with Web.....	26
4-7 - Sample of the Orthotropic Web	28
4-8 - Web Spread on the Floor	29
4-9 - Stress v/s Strain Showing E in MD = 12412	30
4-10 - Web Mounted on Instron UTM	31
4-11 - Stress v/s Strain Showing E in CMD =1580 Psi.....	32
5-1 - Step Amplitude in Abqus (Isotropic Web)	35
5-2 - Abaqus Simulation Model	36
5-3 - Step Amplitude in Abaqus (Orthotropic Web)	37

Figure	Page
6-1 - Experimental Results for the Isotropic Web at a Strain Level of 0.0028	38
6-2 - Experimental Results for the Isotropic Web at a Strain Level of 0.0046	39
6-3 - Experimental Results for the Isotropic Web at a Strain Level of 0.0081	39
6-4 - Repeatability Tests for Troughs in the Isotropic Web at a Strain Level of 0.0028.....	40
6-5 - Repeatability Tests for Troughs in the Isotropic Web at a Strain Level of 0.0046.....	40
6-6 - Repeatability Tests for Troughs in the Isotropic Web at a Strain Level of 0.0081.....	41
6-7 - Depicting the Estimation of Wavelength and Amplitude (Experiment Results)	41
6-8 - Experimental Results of Wavelength on the Isotropic Web (in)	42
6-9 - Experimental Results of Amplitude on the Isotropic Web (in)	43
6-10 - Depicting the Estimation of Wavelength and Amplitude (Abaqus Results).....	44
6-11 - Abaqus Results for the Isotropic Web at a Strain Level of 0.0028.....	44
6-12 - Abaqus Results for the Isotropic Web at a Strain Level of 0.0046.....	45
6-13 - Abaqus Results for the Isotropic Web at a Strain Level of 0.0081.....	45
6-14 - Comparison of Wavelength with Theoretical Results on the Isotropic Web.....	46
6-15 - Comparison of Amplitude with Theoretical Results on the Isotropic Web.....	47
6-16 - CMD Compressive Stresses at a MD Strain Level of 0.0012 (in/in).....	48
6-17 - Image From Zheng[10] Showing Amplitude Results	49
6-18 - Experimental Results for the Orthotropic Web at a Strain Level of 0.006.....	50
6-19 - Experimental Results for the Orthotropic Web at a Strain Level of 0.012.....	50
6-20 - Experimental Results for the Orthotropic Web at a Strain Level of 0.018.....	50
6-21 - Repeatability Tests for Troughs in Orthotropic Web at a Strain Level of 0.006	51
6-22 - Repeatability Tests for Troughs in Orthotropic Web at a Strain Level of 0.012	51
6-23 - Repeatability Tests for Troughs in Orthotropic Web at a Strain Level of 0.018	51
6-24 - Depicting the Estimation of Wavelength and Amplitude (Experiment Results)	52

Figure	Page
6-25 - Experimental Results of Wavelength on the Orthotropic Web.....	53
6-26 - Experimental Results of Amplitude on the Orthotropic Web.....	53
6-27 - CMD compressive Stresses at a MD Strain Level of 0.018.....	54
6-28 - Picture Depicting Non-Uniform Thickness in the Orthotropic Web	55
6-29 - Out-of-plane Displacement Associated with the Web Shown in Figure 6-28.....	56
6-30 - Comparison of Experiment and Theoretical Wavelength on Orthotropic Web.....	57
6-31 - Comparison of Experiment and Theoretical Amplitude on Orthotropic Web.....	57
6-32 - Depicting the Measurement of Wavelength and Amplitude (Abaqus Results)	58
6-33 - Abaqus Results for the Orthotropic Web at a Strain Level of 0.0034	59
6-34 - Abaqus Results for the Orthotropic Web at a Strain Level of 0.0063	59
6-35 - CMD Stresses in the Orthotropic Web (Pseudo Material).....	60
6-36 - CMD Stresses in the Orthotropic Web with Refined Scale (Pseudo Material)	60
6-37 - Comparison of Abaqus and Theoretical Wavelength on the Orthotropic Web	61
6-38 - Comparison of Abaqus and Theoretical Amplitude on the Orthotropic Web	62
A-1 - Repeatability Test for Troughs in the Isotropic Web at a Strain Level of 0.0012	67
A-2 - Repeatability Test for Troughs in the Isotropic Web at a Strain Level of 0.0017	67
A-3 - Repeatability Test for Troughs in the Isotropic Web at a Strain Level of 0.0023	68
A-4 - Repeatability Test for Troughs in the Isotropic Web at a Strain Level of 0.0035	68
A-5 - Repeatability Test for Troughs in the Isotropic Web at a Strain Level of 0.0041	68
A-6 - Repeatability Test for Troughs in the Isotropic Web at a Strain Level of 0.0052	69
A-7 - Repeatability Test for Troughs in the Isotropic Web at a Strain Level of 0.0058	69
A-8 - Repeatability Test for Troughs in the Isotropic Web at a Strain Level of 0.0064	69
A-9 - Repeatability Test for Troughs in the Isotropic Web at a Strain Level of 0.0069	70
A-10 - Repeatability Test for Troughs in the Isotropic Web at a Strain Level of 0.0075	70

A-11 - Abaqus Results of Troughs on Isotropic Web at a Strain Level of 0.0035	70
A-12 - Abaqus Results of Troughs on Isotropic Web at a Strain Level of 0.0041	71
A-13 - Abaqus Results of Troughs on Isotropic Web at a Strain Level of 0.0052	71
A-14 - Abaqus Results of Troughs on Isotropic Web at a Strain Level of 0.0058	71
A-15 - Abaqus Results of Troughs on Isotropic Web at a Strain Level of 0.0064	72
A-16 - Abaqus Results of Troughs on Isotropic Web at a Strain Level of 0.0069	72
A-17 - Abaqus Results of Troughs on Isotropic Web at a Strain Level of 0.0075	72
A-18 - Repeatability Tests for Troughs in Orthotropic Web at a Strain Level 0.009	73
A-19 - Repeatability Tests for Troughs in Orthotropic Web at a Strain Level 0.015	73

CHAPTER I

INTRODUCTION

An Introduction to Webs

A web is a material that is very long compared to its width. Webs are usually quite thin compared to their width dimension and are stored and transported in the form of rolls. Webs are often subjected to several continuous processes in which value is added prior to manufacturing a final product. During these processes the web is first unwound and then transported over a series of rollers, some of which are driven and others not, through the process and then finally rewound to await the next process. The objective is to transport these webs through processes with minimal defects and economic loss. Transport of a web through a process machine is accomplished by driving some of the rollers in the process machine.

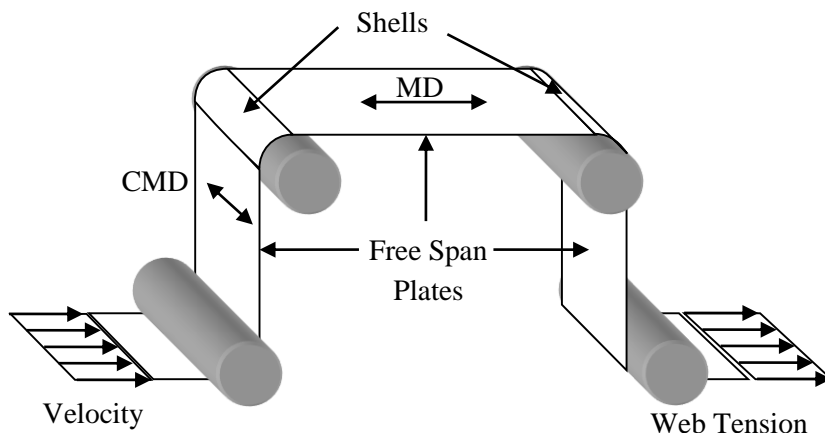


Figure 1-1 - A Web Travelling Through a Process Machine

To achieve good transport conditions where the web is laterally located properly and flat for proper processing requires the web to be under tension as shown in Figure 1-1. This tension is achieved by increasing the velocity of the driven rollers successively through the web line and via frictional forces between these rollers and the web.

Web Instability

As the web travels through a process machine it moves in the Machine Direction (MD) shown in Figure 1-1. The direction orthogonal to the MD but still within the plane of the web is called the Cross Machine Direction (CMD). Due to the small thickness of the web, the bending stiffness of the web is also small, and web tension is often sufficient to make the web take the shape of the roller surface as the web transits the roller. Thus the shape of the web on the roller is a sector of a cylindrical shell. The unsupported web between rollers is called a free span. In good processing conditions this web has the form of a flat plate. Often web instability can be witnessed in free spans as shown in Figure 1-2. These instabilities are called web troughs. Sometimes if the amplitude of the troughs becomes large enough a secondary instability called a wrinkle, shown in Figure 1-3 will form on rollers.

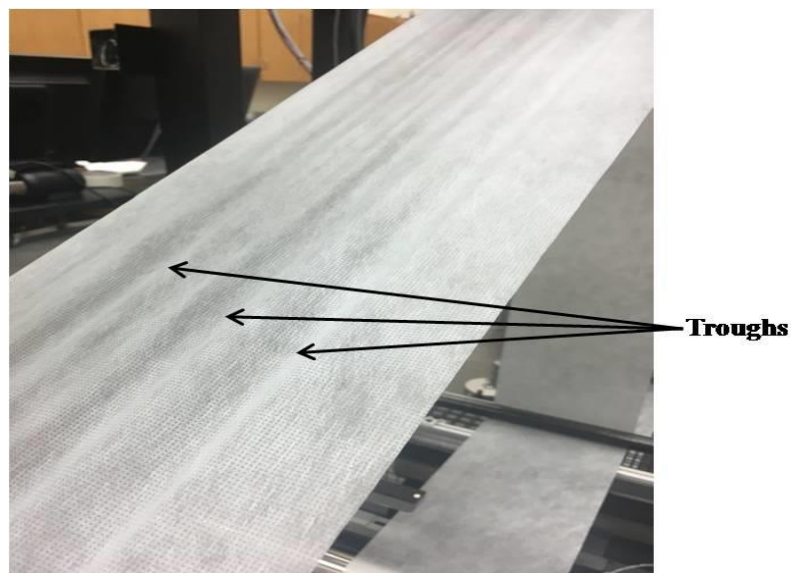


Figure 1-2 - Web Trough Instability

Web troughs form as a result of small CMD compressive stresses that may result from imperfections in the web or the rollers and often the source of the stress is unknown. In some cases the troughs are considered benign as they may not cause harm in free spans where web processing is occurring. Web processes such as coating or printing require the web to be as flat as possible.

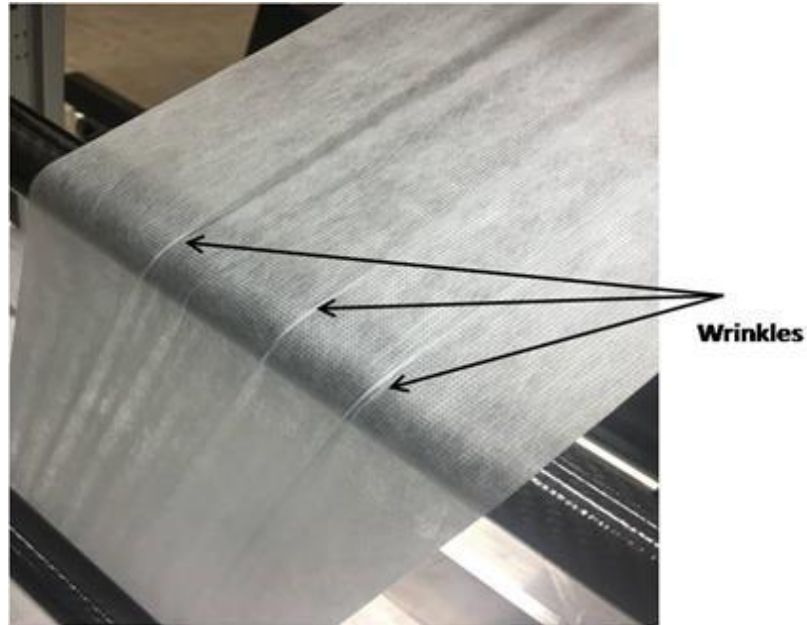


Figure 1-3 Web Wrinkles on Rollers

Wrinkles are undesirable as they almost always result in inelastic deformation or fracture of the web. The CMD compressive stresses required to induce wrinkles in web shells on rollers are often two to three orders of magnitude larger than the stresses required to form troughs. The stability of the web in shell form is much larger than the stability of the web in plate form. Wrinkles have been found to be precipitated by troughs. Beisel et al [1] demonstrated that roller misalignment can induce troughs and that higher misalignments can induce wrinkles. Beisel also proved that troughs could be predicted with closed form linear buckling theory but that prediction of wrinkles required nonlinear post buckling analyses.

The Theory of Inextensibility

Cerda et al [2] [3] developed a theory of inextensibility to predict the amplitude of the out-of-plane deformation of troughs. This theory is based on the assumption that the CMD stresses are so low that the CMD strains are governed by web tension, Young's modulus and Poisson's ratio. The width reduction associated with the CMD strain would result in out-of-plane trough deformation. The benefit of this work is a closed form algorithm for trough amplitude was realized that could potentially be useful to those who transport webs through web process machinery. A limitation was that the theory of inextensibility does not consider the pre-buckled state of the web before troughs have formed. It is also assumed that the web width reduction due to the Poisson effect is the only disturbance which causes the out-of-plane deformation.

This Research

A closed form expression to predict trough amplitude could be very useful. Many webs have orthotropic material properties. The focus of this thesis will be to extend the theory of inextensibility to orthotropic webs and to verify the theory for elastic isotropic and orthotropic web materials. Verification will be achieved in laboratory tests and using nonlinear finite element simulation.

CHAPTER II

LITERATURE SURVEY

The wavelength of the troughs will be necessary in prediction of the troughs amplitudes.

Wavelength of Troughs on Isotropic Webs

The instability of webs is equivalent to the instability of thin plates with little bending stiffness. Consider an isotropic rectangular plate of length 'a', width 'b' and thickness 't' subjected to tensile stress σ_x in MD and tensile stress σ_y in CMD as shown in Figure 2-1.

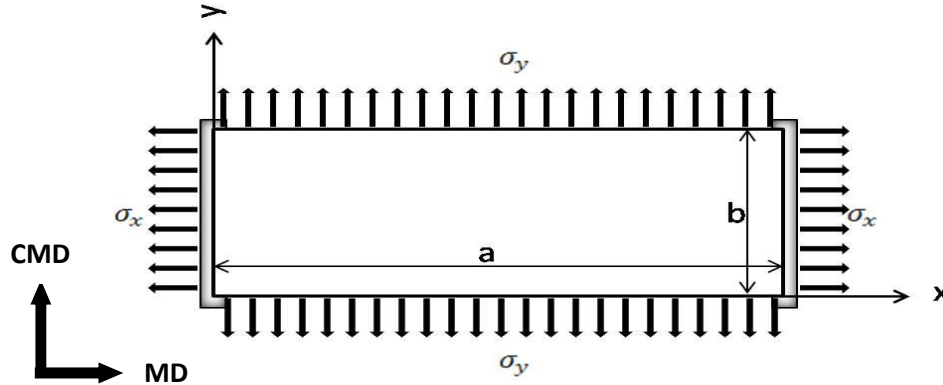


Figure 2-1 - Rectangular Plate under Biaxial Stress with Simply Supported Edges

The above plate is in a plane stress state, which means $\sigma_z = 0$. Let u , v be the displacements in x and y directions respectively. Let $w(x, y)$ be the out-of-plane displacement of a rectangular plate. For an isotropic rectangular plate subjected to biaxial load, the out-of-plane deformation is governed by the following differential equation [4],

$$\frac{\partial^4 w}{\partial x^4} + 2 \frac{\partial^4 w}{\partial x^2 \partial y^2} + \frac{\partial^4 w}{\partial y^4} = \frac{1}{D} \left(\sigma_x t \frac{\partial^2 w}{\partial x^2} + \sigma_y t \frac{\partial^2 w}{\partial y^2} \right) \quad (1)$$

Where, $D = \frac{Et^3}{12(1-\nu^2)}$, E is the Young's modulus and ν is Poisson's ratio.

The equation (1) can be rewritten as,

$$D \frac{\partial^4 w}{\partial x^4} + 2D \frac{\partial^4 w}{\partial x^2 \partial y^2} + D \frac{\partial^4 w}{\partial y^4} - \left(\sigma_x t \frac{\partial^2 w}{\partial x^2} + \sigma_y t \frac{\partial^2 w}{\partial y^2} \right) = 0 \quad (2)$$

To predict the minimum compressive stress in CMD required for the formation of troughs, Good and Biesel [5] assumed a double sine function for the displacement surface in out-of-plane direction of the form,

$$w(x, y) = A_{mn} \sin\left(\frac{m\pi x}{a}\right) \sin\left(\frac{n\pi y}{b}\right) \quad (3)$$

Where, A_{mn} is the maximum amplitude of the displacement surface, m and n are positive integers given by the half wave numbers in MD and CMD respectively. The assumption of the out-of-plane displacement surface given by equation (3) satisfies simply supported boundary conditions $w(0, y) = w(a, y) = w(x, 0) = w(x, b) = 0$. The half wave number, m in MD is equal to one because of the assumption that the web will be subjected to tension in the MD on x-direction. The simply support boundary conditions for the plate in Figure 2-1 were deemed appropriate because the rollers and web tension prevent out-of-plane web displacement at the rollers. Furthermore, the σ_y stresses shown in Figure 2-1 must be zero due to surface equilibrium. Non-zero σ_y stresses can develop between the web edges however. With the absence of σ_y stresses at the horizontal boundaries and the presence of the σ_x stresses due to web tension, it was assumed the out-of-

plane displacement (w) would be minimal on the horizontal boundaries as well. Thus, simple supports were assumed for all boundaries.

Now, substituting equation (3) into equation (2) and solving for compressive stress σ_y . We get a relationship for the CMD (σ_y) stresses in the form,

$$\sigma_y = -\left(\frac{\sigma_e(a^2n^2 + b^2)^2 + \sigma_x b^4}{n^2 a^2 b^2}\right) \quad (4)$$

Where, $\sigma_e = \frac{\pi^2 D}{a^2 t}$. From equation (4) we can say that σ_y is a function of the half wave number, n and tensile stress σ_x . Also, σ_y is directly proportional to the magnitude of tensile stress σ_x . Good and Beisel [6] considered the concept of minimum energy to find the exact positive integer value of half wave number in CMD, n for a given magnitude of tensile stress. With a temporary assumption that n is continuous, the derivative of equation (4) with respect to n is set equal to zero. Solving that expression to zero yields:

$$n = \frac{b}{a} \left(\frac{\sigma_x}{\sigma_e} + 1\right)^{\frac{1}{4}} \quad (5)$$

To be exact, the value of n should then be rounded to the nearest positive integer, such that upon substitution into equation (3) the simply supported boundary condition is enforced ($w = 0$) when $y = 0$ and when $y = b$. However, by leaving n continuous a convenient approximation for the critical buckling stress $\sigma_{y,cr}$ can be obtained. Substitution of equation (5) into (4) yields:

$$\sigma_{y,cr} \approx -2\left(\sqrt{\sigma_e \sigma_x + \sigma_e^2} + \sigma_e\right) \quad (6)$$

In Figure 2-1, positive σ_x and σ_y stresses are shown acting on the plate as assumed by Timoshenko [4] in the development of the differential equation for the out-of-plane displacement, $w(x, y)$. The negative sign in equation (6) indicates that a compressive σ_y stress is needed to induce troughs in the web. Good and Beisel [6] found through substitution of typical web thickness, span dimensions and material properties into σ_e that σ_e is very small in comparison to the σ_x stresses resulting from web tension. This allows equation (6) simplified to,

$$\sigma_{y,cr} \approx -2\sqrt{\sigma_x \sigma_e} = -\frac{\pi t}{a} \left(\frac{E \sigma_x}{3(1-\nu^2)} \right)^{\frac{1}{2}} \quad (7)$$

Examination of equation (7) indicates that thin webs in long free spans with low modulus can with stand very little σ_y compressive stress prior to trough formation. It also indicates that the web tension which induces the σ_x stress is a stabilizing influence on the web. If the σ_x stress is increased on the web, more σ_y compressive stress is required to induce trough instability.

The wavelength, λ can be found by dividing the total width of the web by the number of troughs in the web. It can be estimated by noting for typical web parameters that $\frac{\sigma_x}{\sigma_e} \gg 1$:

$$\lambda = \frac{b}{n/2} = \frac{2b}{INT \left(\frac{b}{a} \left(\frac{\sigma_x}{\sigma_e} + 1 \right)^{\frac{1}{4}} \right)} \approx \frac{2a}{\sqrt[4]{1 + \frac{\sigma_x}{\sigma_e}}} \approx \frac{\sqrt{2\pi a t}}{\sqrt[4]{\frac{3\sigma_x(1-\nu^2)}{E}}} \quad (8)$$

The wavelength is independent of width b. If the stress in CMD is more compressive than the stress given by equation (7), the web begins to buckle into troughs.

Wavelength of Troughs on Orthotropic webs

For an Orthotropic rectangular plate subjected to biaxial load, the out-of-plane displacement curve is given by Lekhnitskii, S.G [7].,

$$D_1 \frac{\partial^4 w}{\partial x^4} + 2D_3 \frac{\partial^2 w}{\partial x^2} \frac{\partial^2 w}{\partial y^2} + D_2 \frac{\partial^4 w}{\partial y^4} = \sigma_x t \frac{\partial^2 w}{\partial x^2} + \sigma_y t \frac{\partial^2 w}{\partial y^2} \quad (9)$$

$$\text{Where, } D_1 = \frac{E_x t^3}{12(1-\nu_{xy}\nu_{yx})}; D_2 = \frac{E_y t^3}{12(1-\nu_{xy}\nu_{yx})}; D_3 = D_1 \nu_{xy} + 2D_k; D_k = \frac{Gt^3}{12} \quad (10)$$

Here, E_x and E_y are Young's modulus of orthotropic web in MD and CMD respectively per Figure 2-1. G is the shear modulus of the web. Constitutive relations between stress and strain define the Poisson's ratios by following equations:

$$\begin{pmatrix} \varepsilon_x \\ \varepsilon_y \\ \gamma_{xy} \end{pmatrix} = \begin{pmatrix} \frac{1}{E_x} & \frac{-\nu_{yx}}{E_y} & 0 \\ \frac{-\nu_{xy}}{E_x} & \frac{1}{E_y} & 0 \\ 0 & 0 & \frac{1}{G_{xy}} \end{pmatrix} \begin{pmatrix} \sigma_x \\ \sigma_y \\ \tau_{xy} \end{pmatrix} \quad (11)$$

It is assumed that E_x and E_y are the principal moduli and that they are aligned with the x and y directions respectively. The Poisson's ratio ν_{xy} couples the strain induced in the y (CMD) direction due a stress applied in the x (MD) direction. Similarly, principal Poisson's ratio ν_{yx} couples the strain induced in the x (MD) direction due to a stress applied in the y (CMD) direction. Among the 5 constants ($E_x, E_y, \nu_{xy}, \nu_{yx}, G_{xy}$) only four of them are independent since

the Maxwell's relation dictates, $\frac{\nu_{yx}}{E_y} = \frac{\nu_{xy}}{E_x}$.

Substituting equation (3) into equation (9) using $m=1$, yields,

$$\frac{\pi^2 \sqrt{D_1 D_2}}{a^2 t} \left(\sqrt{\frac{D_1}{D_2}} + 2 \left(\frac{an}{b} \right)^2 \frac{D_3}{\sqrt{D_1 D_2}} + \left(\frac{an}{b} \right)^4 \sqrt{\frac{D_2}{D_1}} \right) + \sigma_x + \left(\frac{an}{b} \right)^2 \sigma_y = 0 \quad (12)$$

Simplifying the equation (12) for σ_y we get,

$$\sigma_y = - \left(\frac{b}{an} \right)^2 \left\{ \sigma_{eo} \left[\sqrt{\frac{D_1}{D_2}} + 2 \left(\frac{an}{b} \right)^2 \frac{D_3}{\sqrt{D_1 D_2}} + \left(\frac{an}{b} \right)^4 \sqrt{\frac{D_2}{D_1}} \right] + \sigma_x \right\} \quad (13)$$

Where, $\sigma_{eo} = \frac{\pi^2 \sqrt{D_1 D_2}}{a^2 t}$.

Good and Beisel [6] in a derivation similar to that for the wavelength of troughs on isotropic webs, used the theory of minimum energy to find the positive integer value for the half wave number in the CMD, n for a given magnitude of tensile stress. With the assumption that n is temporarily continuous, derivative of equation (13) is taken with respect to n and set to zero. That equation is then solved for n :

$$n = \frac{b}{a\sqrt{\pi}} \left(\frac{\pi^2 D_1 + a^2 t \sigma_x}{D_2} \right)^{\frac{1}{4}} = \frac{b}{a} \sqrt[4]{\left(\frac{D_1}{D_2} + \frac{a^2 t \sigma_x}{\pi^2 D_2} \right)} \quad (14)$$

Similar to the derivation for the isotropic web n should be rounded to the nearest positive integer to be exact such that equation (3) will satisfy the simply supported boundary conditions. However, there is benefit to allowing n to remain continuous until the critical buckling stress is determined and reduced.

The equation for the critical compressive stress $\sigma_{y,cr}$ for an orthotropic web was determined by substituting equation (14) into equation (13) given by:

$$\sigma_{y,cr} = -\frac{2\pi}{a^2t} \left[\frac{\left(\pi^2 D_1 \sqrt{D_2} + a^2 t \sigma_x \sqrt{D_2} + \pi D_3 \sqrt{\pi^2 D_1 + a^2 t \sigma_x} \right)}{\sqrt{\pi^2 D_1 + a^2 t \sigma_x}} \right] \quad (15)$$

In a parametric study where typical web values for t , a , σ_x , E_x , E_y , ν_{xy} and ν_{yx} were varied, Good and Beisel [5] found the $\pi^2 D_1$ term was there to four orders of magnitude less than the $ta^2 \sigma_x$ term. This allowed simplification of equations (14) and (15) to:

$$n = \frac{b}{a\sqrt{\pi}} \left(\sqrt[4]{\frac{a^2 t \sigma_x}{D_2}} \right) = b \left(\sqrt{\frac{2}{\pi a t}} \right) \left(\sqrt[4]{\frac{3(1-\nu_{xy}\nu_{yx})\sigma_x}{E_y}} \right) \quad (16)$$

And,

$$\sigma_{y,cr} \approx -\frac{\pi t}{a} \left(\sqrt{\frac{\sigma_x E_y}{3(1-\nu_{xy}\nu_{yx})}} \right) \quad (17)$$

Similarly, the wavelength λ can be found by dividing total width of the web by number of troughs in the web given by,

$$\lambda = \frac{b}{n/2} = \frac{2b}{INT \left[b \sqrt{\frac{2}{\pi a t}} \sqrt[4]{\frac{3(1-\nu_{xy}\nu_{yx})\sigma_x}{E_y}} \right]} \approx \frac{\sqrt{2ah\pi}}{\sqrt[4]{3\sigma_x(1-\nu_{xy}\nu_{yx})}} \quad (18)$$

The equation of wavelength is independent of width b . If the stress in CMD is more compressive than the stress given by equation (18), the web begins to buckle.

Amplitude of Troughs on Isotropic Web

E. Cerda and L. Mahadevan [2], [3] developed an equation for amplitude of wrinkles (he refers troughs as wrinkles) on an isotropic web using ‘‘The Condition of Inextensibility’’. Let a rectangular web of length ‘ L ’, width ‘ W ’ and thickness ‘ t ’ ($L > W \gg t$) clamped at two edges is subjected to longitudinal strain γ . The web with Young’s Modulus ‘ E ’ and Poisson’s Ratio ‘ ν ’ is observed to be remain flat until longitudinal strain is less than the critical stretching strain γ_{cr} . If

the web is subjected to longitudinal strain greater than the critical stretching strain γ_{cr} , it leads to the formation of wrinkles. E. Cerda and L. Mahadevan [3] claim that the web does not undergo lateral displacement at fixed ends due to the boundary constraints.

To derive an accurate expression for wavelength and amplitude he considered changes in bending energy and stretching energy given by total energy function. He used a Lagrange multiplier (L) to account energy for geometric constraint. Total energy function is given by expression,

$$U = U_B + U_s + L \quad (19)$$

Where, U_B is the bending energy, U_s is the stretching energy and L is the Lagrange Multiplier.

He assumed the out-of-plane displacement of the web as $w(x, y)$, $x \in (0, 1)$ and $y \in (0, W)$. The expression for bending energy is given by,

$$U_B = \frac{1}{2} \int_x \int_y D \left(\frac{\partial^2 w}{\partial y^2} \right)^2 dx dy \quad (20)$$

Where, $D = \frac{Et^3}{12(1-\nu^2)}$.

The expression for stretching energy is given by,

$$U_s = \frac{1}{2} \int_x \int_y T(x) \left(\frac{\partial w}{\partial x} \right)^2 dx dy \quad (21)$$

Where $T(x)$ is the tension in the direction of x .

Now, Authors introduced the term ‘‘Condition of Inextensibility’’ which implies that the width of the sheet is conserved in the process of formation of wrinkles.

The reduced width of the elastic sheet due to the out-of-plane displacement is given by,

$$W' = \int_0^w \left[1 - \frac{1}{2} \left(\frac{\partial w}{\partial y} \right)^2 \right] dy \quad (22)$$

The reduced width of the web due to Poisson's effect is given by,

$$W' = \int_0^w (1 - \nu\gamma) dy \quad (23)$$

By equating the equation (22) and equation (23), we can write the "Condition of Inextensibility" as,

$$\int_0^w \left(\frac{1}{2} \left(\frac{\partial w}{\partial y} \right)^2 - \frac{\Delta}{W} \right) dy = 0 \quad (24)$$

Where, $\Delta(x)$ is the displacement due to compressive force in transverse direction equal to the product of strain in that direction and width W . Therefore, $\Delta(x) = \nu\gamma W$. The expression for Lagrange Multiplier in equation (19) is,

$$L = - \int \int_{x y} c(x) \left[\frac{1}{2} \left(\frac{\partial w}{\partial y} \right)^2 - \frac{\Delta}{W} \right] dx dy \quad (25)$$

Where, $c(x)$ is an unknown Lagrange multiplier.

Substituting equation (20), equation (21) and equation (25) into total energy function given by equation (19) we get,

$$U = \frac{1}{2} \int \int_{x y} D \left(\frac{\partial^2 w}{\partial y^2} \right)^2 dx dy + \frac{1}{2} \int \int_{x y} T(x) \left(\frac{\partial w}{\partial x} \right)^2 dx dy - \int \int_{x y} c(x) \left[\frac{1}{2} \left(\frac{\partial w}{\partial y} \right)^2 - \frac{\Delta}{W} \right] dx dy \quad (26)$$

We obtain Euler-Lagrange equation by minimizing the total energy function given by equation (26) with respect to w ,

$$D \frac{\partial^4 w}{\partial y^4} - T(x) \frac{\partial^2 w}{\partial x^2} + b(x) \frac{\partial^2 w}{\partial y^2} = 0 \quad (27)$$

In equation (27), tension $T(x)$ is constant given by the product of stress and thickness t equal to Ety , while $\Delta(x) = \nu\gamma W$ is a constant far from the clamped boundaries, so that $c(x)$ is a constant. The boundary conditions near the clamped edges are as follows,

$$w(0, y) = w(L, y) = 0 \quad (28)$$

He assumed a periodic solution for out of plane displacement $w(x, y) = \sum_n e^{ik_n y} X_n(x)$ where,

$k_n = \frac{2\pi n}{W}$ and substituted it in equation (27), which gives a Sturm-Liouville problem,

$$\frac{d^2 X_n}{dx^2} + \left(\frac{ck_n^2 - Bk_n^4}{T} \right) X_n = 0, \quad (29)$$

$$X_n(0) = X_n(L) = 0$$

Now, write $\left(\frac{ck_n^2 - Bk_n^4}{T} \right) = \omega_n^2$. Solution to equation (29) can be written in the form of,

$$X_n = A_n \text{Sin } \omega_n x \quad (30)$$

Where, $\omega_n = \frac{m\pi}{L}$. The half wave number, m is restricted to unity to minimize the bending energy, therefore

$$\frac{\pi^2}{L^2} = \frac{ck_n^2 - Dk_n^4}{T} \quad (31)$$

Equation (31) is rearranged as $c = \frac{\pi^2 T}{L^2 k_n^2} + Dk_n^2$. Using equation (30), the solution for

displacement function $w(x, y)$ is given by,

$$w(x, y) = A_n \text{Cos}(k_n y + \phi_n) \text{Sin}\left(\frac{\pi x}{L}\right) \quad (32)$$

Cerda assumes a simple support as well by selecting the Sine term in equation (32).

Substituting equation (32) into equation (24) gives,

$$\Delta = \frac{A_n^2 k_n^2 W}{8} \quad (33)$$

Substituting equation (32) into equations of bending energy (20) and stretching energy (21), and then substituting them back to total energy function we get,

$$U = D k_n^2 \Delta L + \frac{\pi^2 T \Delta}{k_n^2 L} \quad (34)$$

The equation of wavelength can be derived by minimizing equation (34) with respect to k_n ,

$$\lambda = 2\sqrt{\pi} \sqrt[4]{\frac{D}{T}} \sqrt{L} \quad (35)$$

The equation of amplitude can be derived by substituting the result in the condition of inextensibility along y,

$$\int_0^b \left[\frac{1}{2} \left(\frac{\partial w}{\partial y} \right)^2 - \frac{\Delta}{W} \right] dy = 0 \quad (36)$$

The equation of amplitude is given by,

$$A = \frac{1}{\pi} \sqrt{\frac{2\Delta}{W}} \lambda \quad (37)$$

Substituting back the equation for flexural rigidity $D = \frac{Et^3}{12(1-\nu^2)}$, tensile stress $T = Et\gamma$, and

transverse displacement $\Delta = \nu\gamma W$ into equation (35) and equation (37) we get,

Wavelength,

$$\lambda = \frac{\sqrt{2\pi Lt}}{\sqrt[4]{3\gamma(1-\nu^2)}} \quad (38)$$

The wavelength given by equation (38) is equivalent to equation (8).

Amplitude,

$$A = \frac{\sqrt{4\nu t L \sqrt{\gamma}}}{\sqrt[4]{3\pi^2(1-\nu^2)}} \quad (39)$$

To prove the validity of the equations of wavelength and amplitude, E. Cerda and L. Mahadevan [3] conducted experiments on a rectangular polyethylene sheet of length 25cm, width 10cm, thickness 0.01cm clamped at two edges. The Figure 2-2a shows the experimental photograph of wrinkles on elastic sheet conducted by E. Cerda and the Figure 2-2b shows the plot of wavelength results from experiment and equation (38). However, he did not provide experimental results of amplitude of wrinkles though he claims that equation (39) is in good agreement with experiment values.

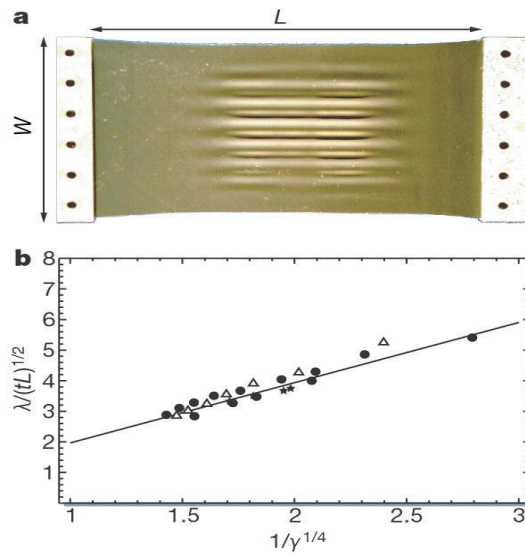


Figure 2-2 - Wrinkles on Polyethylene Sheet

Good [8] employed Cerda's condition of inextensibility to examine the amplitude expression.

The reduced width of the web due to out-of-plane displacement is given by,

$$b' = \int_0^b \left[1 - \frac{1}{2} \left(\frac{\partial w}{\partial y} \right)^2 \right] dy \quad (40)$$

The reduced width of the web due to Poisson's effect is given by,

$$b' = \int_0^b (1 - \nu \gamma) dy \quad (41)$$

Where, γ is strain in MD given by $\frac{\sigma_x}{E}$. By equating the equations (40) and (41), we get the condition of inextensibility given by,

$$\int_0^b \left[\frac{1}{2} \left(\frac{\partial w}{\partial y} \right)^2 - \nu \gamma \right] dy = 0 \quad (42)$$

Substituting equation (3) into equation (42), we can derive an expression for amplitude given by,

$$A = \frac{2a\sqrt{2b\nu\gamma}}{\left[2b\pi\sqrt{\pi^2 + \frac{12a^2\gamma(1-\nu^2)}{t^2}} + a\sqrt{\pi}\sqrt[4]{\pi^2 + \frac{12a^2\gamma(1-\nu^2)}{t^2}} \text{Sin} \frac{2b\sqrt{\pi}}{a}\sqrt[4]{\pi^2 + \frac{12a^2\gamma(1-\nu^2)}{t^2}} \right]^{\frac{1}{2}}} \quad (43)$$

The equation (43) is simplified by eliminating the terms that are of smaller order,

$$A = \sqrt{\frac{2\nu at}{\pi}} \sqrt[4]{\frac{\gamma}{3(1-\nu^2)}} \quad (44)$$

From equation (39) and equation (44), it is clear that the equation of amplitude is not similar. If we go back to his derivations and solve for them in detail, there are few flaws in his derivation.

The equation (33) given by $\Delta = \frac{A_n^2 k_n^2 W}{8}$ is $\Delta = \frac{A_n^2 k_n^2 W}{4}$. From which amplitude is given by

expression $A = \sqrt{\frac{4\Delta}{k_n^2 W}}$. Upon substituting the equation of transverse displacement, $\Delta = v\gamma W$

and equation of wavelength, $\lambda = \frac{\sqrt{2\pi Lt}}{\sqrt[4]{3\gamma(1-v^2)}} = \frac{2\pi}{k}$ we get the final equation of amplitude as,

$$A = \frac{\sqrt{2vtL\sqrt{\gamma}}}{\sqrt[4]{3\pi^2(1-v^2)}} \quad (45)$$

From equation (45) and equation (44), it is clear that the corrected expression for amplitude of troughs given by Cerda et al. and Good are equivalent.

Research Objective

Trough instabilities in webs are a common occurrence in web process machines. Expressions such as (44) and (45) that predict the amplitude of these troughs could be useful if their validity can be proven. Web process engineers can adjust the machine direction strain in the web (γ) and the free span length (a) to reduce the trough amplitude to levels that are acceptable to the process.

The objective of this research will be to study the validity of these amplitude and wavelength expressions through laboratory tests and finite element simulations. Furthermore, the amplitude expressions will be extended to orthotropic webs and the expressions are those for the wavelength (18) will be validated. Limitations of these expressions will be studied.

CHAPTER III

AMPLITUDE OF TROUGHS IN ORTHOTROPIC WEBS

In the following derivation, the principal moduli of an orthotropic web are assumed to be aligned with the x and y directions in Figure 2-1.

Expression for Amplitude of Troughs in Orthotropic Webs

From equation (16) and equation (17), we have critical compressive stress and half wave number, n. We need to write the “Condition of Inextensibility” to derive an expression for amplitude of troughs on orthotropic web. The “Condition of Inextensibility” is defined as the reduced width due to Poisson’s effect is equal to the reduced width due to the out-of-plane displacement.

The reduced width due to Poisson contraction is given by,

$$b' = \int_0^b \left(1 - \frac{\nu_{xy} \sigma_x}{E_x} \right) dy \quad (46)$$

The reduced width due to out-of-plane displacement is given by,

$$b' = \int_0^b \left(1 - \frac{1}{2} \left(\frac{\partial w}{\partial y} \right)^2 \right) dy \quad (47)$$

Equating equations (46) and (47), the condition of inextensibility is written as,

$$\int_0^b \left(\frac{1}{2} \left(\frac{\partial w}{\partial y} \right)^2 - \frac{\nu_{xy} \sigma_x}{E_x} \right) dy = 0 \quad (48)$$

The equation (48) can be simplified as follows,

$$\int_0^b \left(\frac{\partial w}{\partial y} \right)^2 dy = \frac{2b\nu_{xy}\sigma_x}{E_x} \quad (49)$$

Substituting expression for out-of-plane displacement given by equation (3) in equation (49) with half wave number, m restricted to unity, the expression for amplitude is given by,

$$A = \left[\frac{\left(\frac{2b\nu_{xy}\sigma_x}{E_x} \right)^{1/2}}{\frac{b}{2} \left(\frac{n\pi}{b} \right)^2} \right]^{1/2} \quad (50)$$

Where,

$$n = b \sqrt{\frac{2}{\pi at}} \left[\frac{3(1-\nu_{xy}\nu_{yx})\sigma_x}{E_y} \right]^{1/4} \quad (51)$$

By eliminating the terms that are of smaller order in equation (50), the expression for amplitude can be reduced to,

$$A = \sqrt{\frac{2at\nu_{yx}}{\pi}} \sqrt[4]{\frac{\sigma_x/E_y}{3(1-\nu_{xy}\nu_{yx})}} \quad (52)$$

The above equation (52) becomes isotropic equation of amplitude if we input isotropic properties. To prove the validity of the equation of amplitude of troughs on orthotropic web, both the nonlinear finite element software (Abaqus 6.14) and experiment results are compared in next chapters.

CHAPTER IV

EXPERIMENTAL SETUP AND MATERIAL PROPERTIES

Cerda et al [3] performed laboratory tests in which specimens were installed in clamps on the boundaries at $x = 0$ and $x = a$ across the web width. Cerda's tests were performed on polyethylene 0.01 cm or 0.004 inches thick. The boundaries where $y = 0$ and $y = b$ were left free, which is identical to the web edges in free span.

The clamped boundaries appear to contradict the boundary conditions enforced by the displacement functions given by equation (3) and (32). For instance, a clamped boundary constraints both w and $\frac{dw}{dx}$ at $x = 0$ and $x = a$. The simple support boundary conditions enforced by expressions (3) and (32) only constrain w at $x = 0$ and $x = a$. There will be very small moments induced at the boundaries at $x = 0$ and $x = a$ about y -axis due to the clamps. These moments will be very small because the plate bending stiffness will be small for webs which are quite thin.

The clamps are important in these tests because they induce the compressive σ_y stresses that if sufficient will cause the web to buckle and form troughs. Near the clamps the CMD σ_y stresses will be tensile (in the vicinity of $x = 0$ and $x = a$). Away from the clamps ($0 < x < a$) there will be a zone of negative compressive stress which is greater (more negative) than the critical buckling stress will induce troughs.

Figure 3-1 shows the σ_y stresses which resulted from straining a web in the MD between clamped ends.

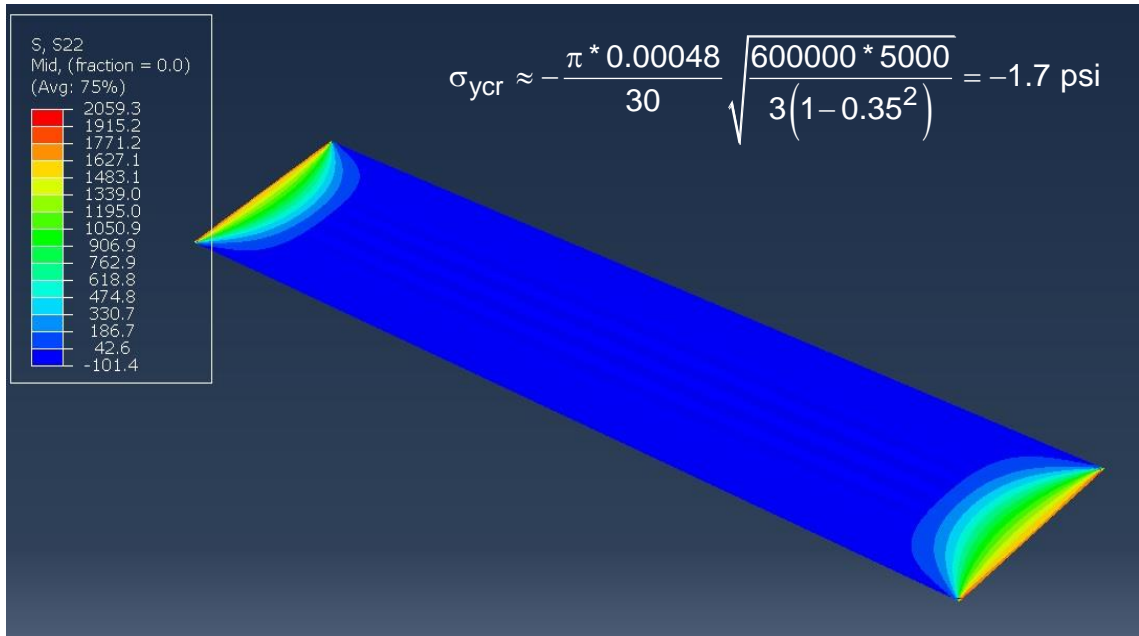


Figure 4-1 - CMD Stresses in a Polyester web, E = 600 Ksi, t = 0.00048", a = 30", b = 6" and $\gamma = 0.008$ in/in.

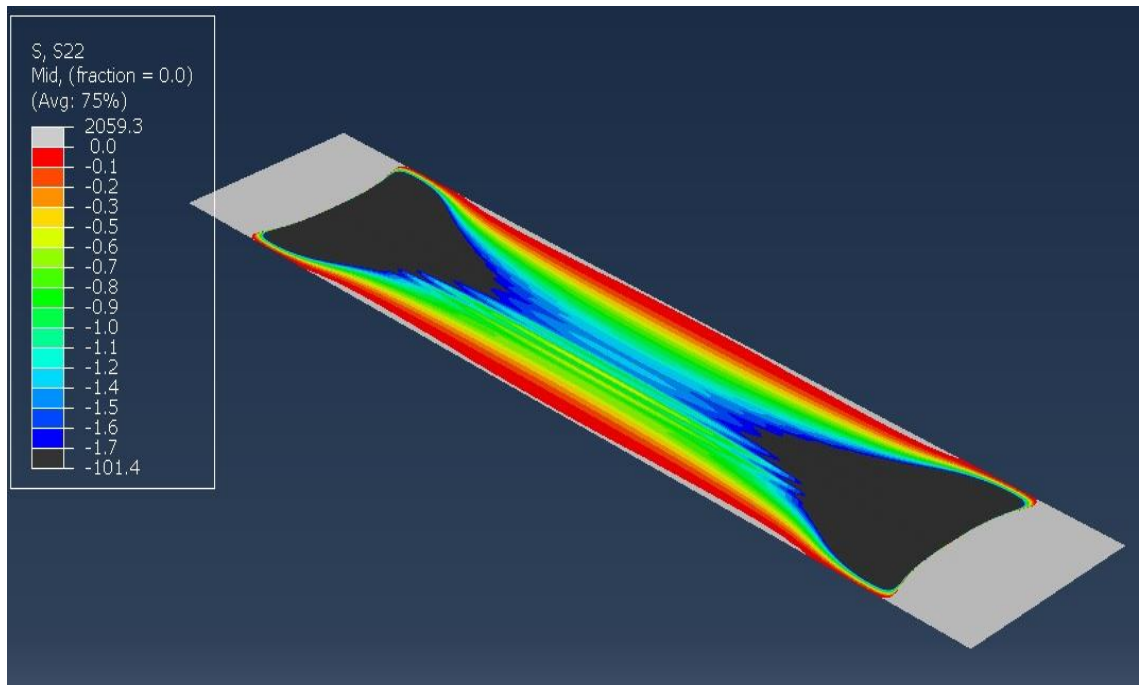


Figure 4-2 – CMD Stresses in a Polyester Web (Refined Scale)

In Figure 4-1, CMD compressive stresses are greater (more negative) than the critical compressive stress of isotropic web given by equation (7). By refining the scale, the compressive stresses greater than the critical compressive stress are as shown in Figure 4-2. The compressive stresses are smaller than the critical compressive stress over much of the span. The troughs we visually witness over the span is due to the CMD compressive stresses that are very localized. The troughs form through the rest of the span at compressive stresses smaller than -1.7 Psi.

The clamped boundaries conditions were chosen for these tests because 1) Cerda used these conditions, 2) These are the simplest boundary conditions that can be enforced on a thin web in the laboratory and 3) The clamped boundary condition should provide the negative σ_y stresses in the web needed to induce troughs.

Experimental Setup to Analyze the Profile of Troughs

The experiments required the use of an Instron Universal Testing Machine, a laser displacement sensor, load cell, a Yo-Yo position pot, data acquisition system, and a user interface to record the profile of troughs. The Web Handling Research Center located at Oklahoma State University, Stillwater provided the equipment, the data acquisition system and the user interface needed for this research.

In this research, the web will be stretched uniformly in the MD and the out-of-plane displacements were measured and recorded at fixed strain levels. An Instron 8502 Universal Testing Machine was used to stretch the web that is clamped at opposite edges. The web is fixed by placing it in between the two aluminum clamps using strong adhesive to avoid slippage of the web from the clamps. After mounting the web between the clamps, a setup to engage the clamps and hold the web between the hydraulic ram of Universal Testing Machine and load cell attached to Instron as shown in Figure 4-3. An additional load cell was attached to the Instron to measure the low load levels acting on the web accurately, as the web is stretched between clamps. A

Keyence model LK-2001 laser sensor was used to capture the out-of-plane displacement of the web under tension. The laser beam of light coming out from laser sensor hits the web in front of it and reflects back to the laser sensor. The distance between the laser sensor and the web is calculated by measuring the time taken by the laser beam to reach the sensor. A Keyence model LK-2001 laser sensor is capable of sensing $1/100000^{\text{th}}$ of inch change in distance. The wavelength and amplitude of troughs formed are calculated from the recorded out-of-plane displacement and position data taken across the width of the web. Hence, to measure the out-of-plane displacement across the width of the web, laser sensor is forced to move horizontally on the linear bearing to capture the out-of-plane displacement at each point along the width. The horizontal position of the laser sensor is measured using an Yo-Yo pot 1850-0500 (motion transducer).

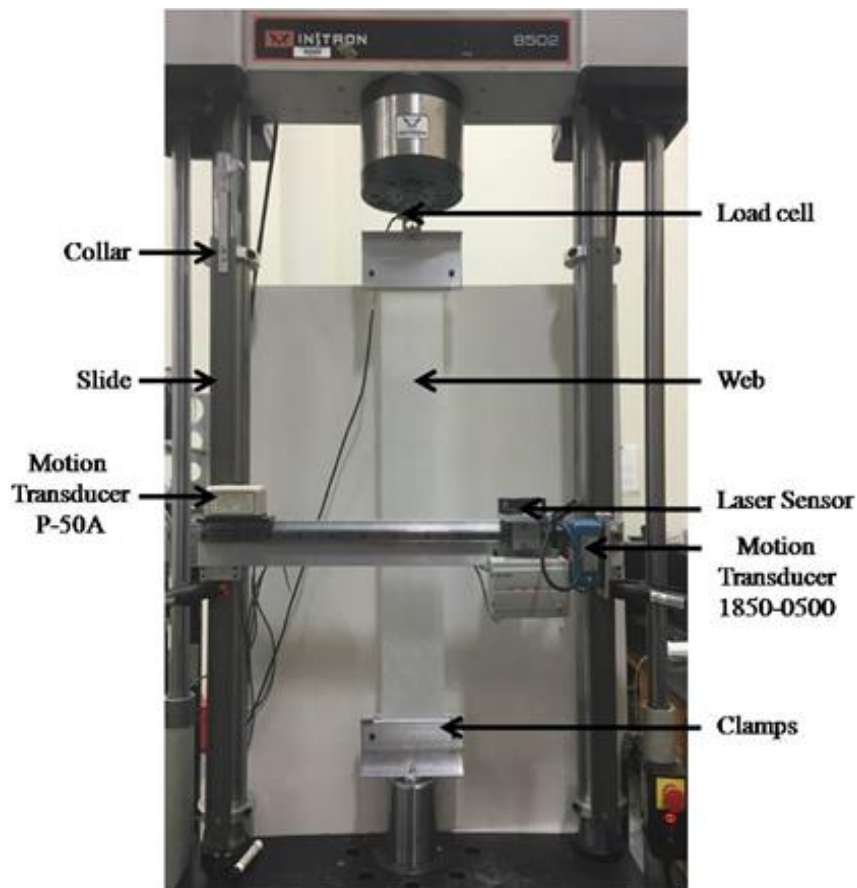


Figure 4-3 - Experimental Setup

Another motion transducer P-50A is used to measure the vertical position of laser sensor. The linear bearing located at the center can be translated vertically using the slide fixed to the arms of Instron. This equipment helps us to capture the profile of troughs on the entire web. The out-of-plane displacement of the web measured from laser sensor, horizontal position of laser sensor measured from Yo-Yo pot 1850-0500 and vertical position of laser sensor measured from motion transducer P-50A is recorded and plotted using the data acquisition system with NI SCB-68 A/O board and a Lab-View program.

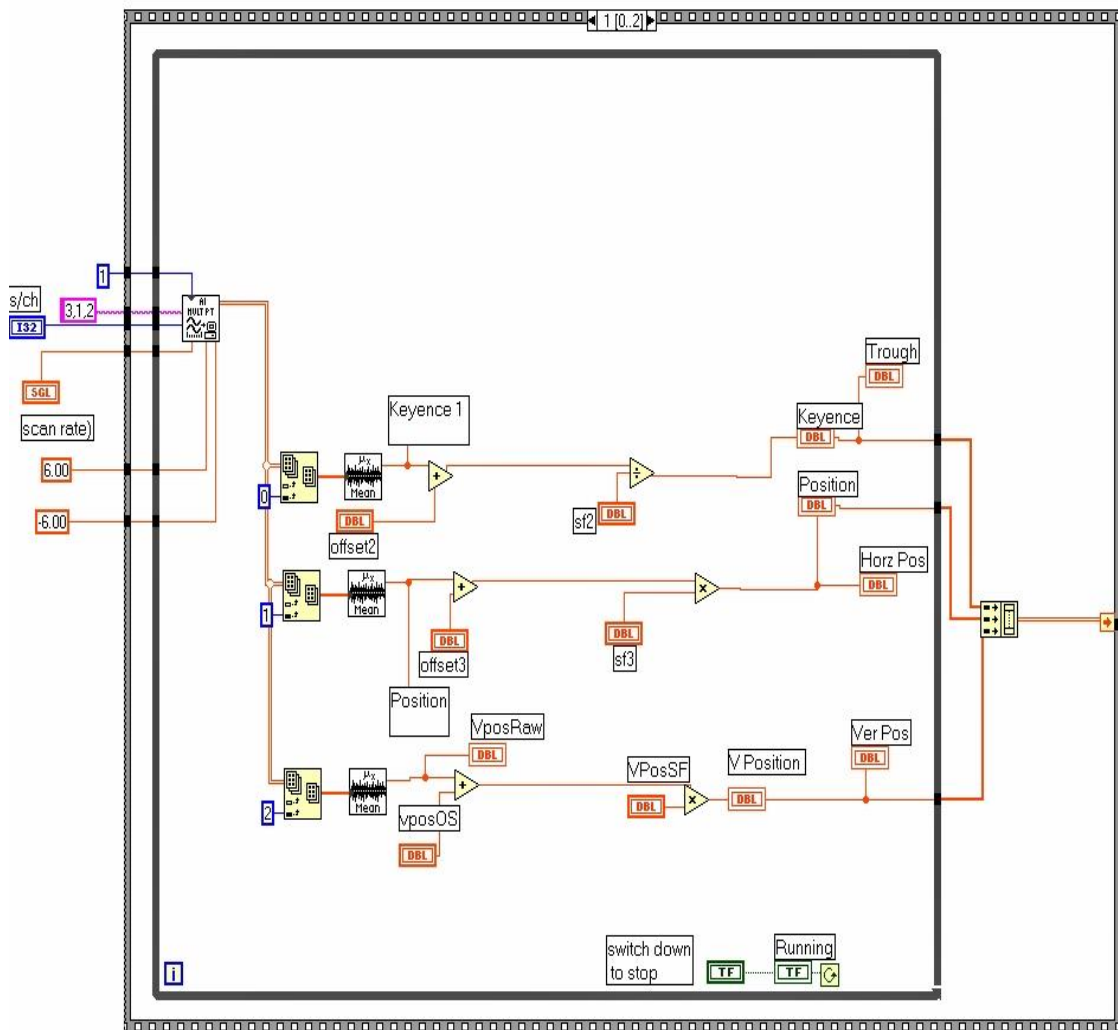


Figure 4-4 - LabView Program

Preparation of Specimens

The aluminum clamps were used to clamp the web at two edges. A splice table was machined to mount the web between aluminum clamps such that the web is orthogonal to the clamps. The Figure 4-5 shows the 30" long splice table.



Figure 4-5 - The Splice Table

A line was scribed on the splice table as a reference to align the web orthogonal to the clamps. The double-sided tape and a strong adhesive were used to fix the web between the clamps. To avoid the slippage of the web, clamps with high friction surface were used. The Figure 4-6 shows the web on the splice table with web fixed between aluminum clamps.



Figure 4-6 - Splice Table with Web

The web fixed at two edges with aluminum clamps is mounted on Instron universal testing machine to analyze the profile of troughs on the web. Uniform load ranging from 2-14 lbs was applied on the web to predict stretch induced troughs on the web. The same experiment was repeated on three different samples of the isotropic web to check the consistency. The average wavelength and amplitude of troughs formed on three samples was used to compare with Abaqus and theoretical results.

An orthotropic web of length 30", width 5" and thickness 0.0055" was tested in the laboratory to study the stretch induced troughs. The web is fixed at both ends following the same procedure discussed above. Uniform load ranging from 2-6 lbs is applied on the web mounted on Instron UTM. The same test is repeated on three different samples of web to analyze the troughs formed due to tension.

Measurement of Material Properties

To validate the expressions for wavelength and amplitude of troughs formed in isotropic and orthotropic web and to run Abaqus simulation, we need to find the material properties of material we are testing in the lab. The material properties of isotropic web include Young's Modulus, Poisson's Ratio, density and the material properties of orthotropic web include thickness, Young's Modulus in MD (E_x) and CMD (E_y), Poisson's Ratio in MD (ν_{xy}), density (ρ) and Shear Modulus G. An isotropic web with known material properties has been picked up from lab to run Abaqus simulations and to conduct tests in lab. DuPont has provided the polyester isotropic web and the material properties. Tests were made to find Young's Modulus in MD and CMD of an orthotropic web. It was difficult to carry out the tests to find the Poisson's ratio because of formation of troughs, hence values given by manufacturers of the web were taken into consideration. Kimberly-Clark Corporation has provided the orthotropic web material as well as the material properties. The Poisson's ratio in MD (ν_{xy}) was given as 1.8.

Isotropic Web Properties (Polyester Web)

The Table 4-1 describes the material properties of an isotropic web.

Length, a	Width, b	Thickness, t	Young's Modulus, E	Poisson's ratio, ν	Density, ρ
30"	6"	0.00048"	600,000 Psi	0.35	0.00013 lb/in ³

Table 4-1 – Material Properties of Polyester Web¹

Thickness of the Orthotropic Web

A 22 g/m² polypropylene spun-bond non-woven web selected as an example of an orthotropic web. A sample of web is shown In Figure 4-7. A variation in fiber density that results in thickness variation is notable in Figure 4-7.



Figure 4-7 - Sample of the Orthotropic Web

A Mitutoyo thickness gauge (model number 2804-F10) was used to find the thickness of the web. The thickness of the web varies across the length and width because of non-uniform nature of web. Hence, several measurements were taken and the average of all of them was taken as the thickness of web. The thickness of the orthotropic web shown in sample is 0.0055 inch.

¹ DuPont provided the polyester web as well as the material properties.

Young's Modulus in MD of Orthotropic Web

A web sample of 600 inch long and 5 inch wide was spread across the hall way as shown in Figure 4-8 to conduct the modulus test of web in the MD. A Shimpo FGV-20 digital force gauge was attached to one end of the web and the opposite side of the web was fixed. A known value of load ranging from 1-6 pounds was applied to the web and the associated increase in length was marked to measure the strain for a known value of stress. An example of data recorded is provided in Table 4-2. The stress and strain are plotted. The slope of the data is the Young's Modulus in MD. This test is repeated four times and the average value was taken as the Young's Modulus in MD.



Figure 4-8 - Web Spread on the Floor

Test data of Young's modulus in MD (Psi)				
Load (lbs)	Stress (psi)	Initial length (in)	Change in Length (in)	Strain (in/in)
1	36	600	1.7	0.0028
2	72	600	3.1	0.0051
3	109	600	4.8	0.0081
4	145	600	6.5	0.0108
5	181	600	8.6	0.0144
6	218	600	11.2	0.0187

Table 4-2 - Test data of Young's Modulus in MD for Test 1

The stress and strain data are shown in Figure 4-9.

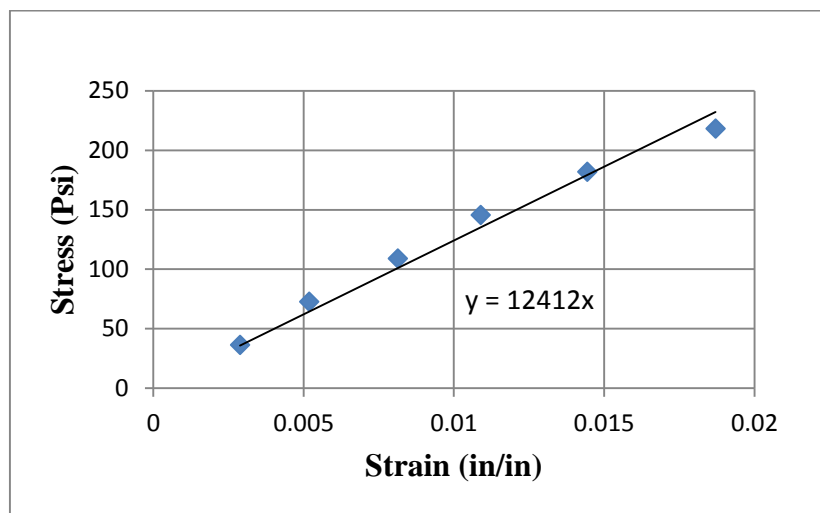


Figure 4-9 - Stress v/s Strain Showing E in MD = 12412

The above test is repeated four times to take the average value as the Young's modulus in MD.

Test	Young's Modulus in MD (Psi)
1	12400
2	12000
3	12200
4	12300
Average	12200

Table 4-3 - Young's Modulus in MD of Four Different Tests

Thus the Young's modulus of orthotropic web in MD was rounded to 12000 Psi.

Young's Modulus in CMD of Orthotropic Web

To find the Young's Modulus in CMD, the sample of web with length 6" was taken from the web roll. Now, the width of the web was considered as length and length was considered as the width to find Young's Modulus in CMD. Hence, the sample was of width 6" and length 5". This sample was fixed on both sides and then mounted on Instron Universal Testing Machine as shown in Figure 4-10 to measure the change in length for known value of stress. After clamping, the length of the web was reduced to 3.9 inches.



Figure 4-10 - Web Mounted on Instron UTM

As the hydraulic ram of the Instron UTM is displaced from its original position the specimen is deformed and subjected to stress. The load and displacement was noted from the user interface of the Instron. Load was converted to stress and the data was recorded in Table 4-4. Hence, Young's Modulus in CMD was estimated by calculating the strain from using change in length associated with the stress applied on the web.

Test Data for Young's Modulus in CMD (Psi)				
Load (lbs)	Stress (psi)	Initial Length (in)	Change in Length (in)	Strain(in/in)
1	30	3.9	0.037	0.0094
1.5	45	3.9	0.063	0.0161
2	60	3.9	0.087	0.0223
2.5	75	3.9	0.121	0.0310
3	90	3.9	0.154	0.0394
3.5	106	3.9	0.188	0.0482
4	121	3.9	0.239	0.0612
4.5	136	3.9	0.287	0.0735
5	151	3.9	0.375	0.0961
5.5	166	3.9	0.41	0.1051
6	181.	3.9	0.493	0.1264

Table 4-4 - Test Data of Young's Modulus in CMD

The stress and strains were plotted as shown in Figure 4-11.

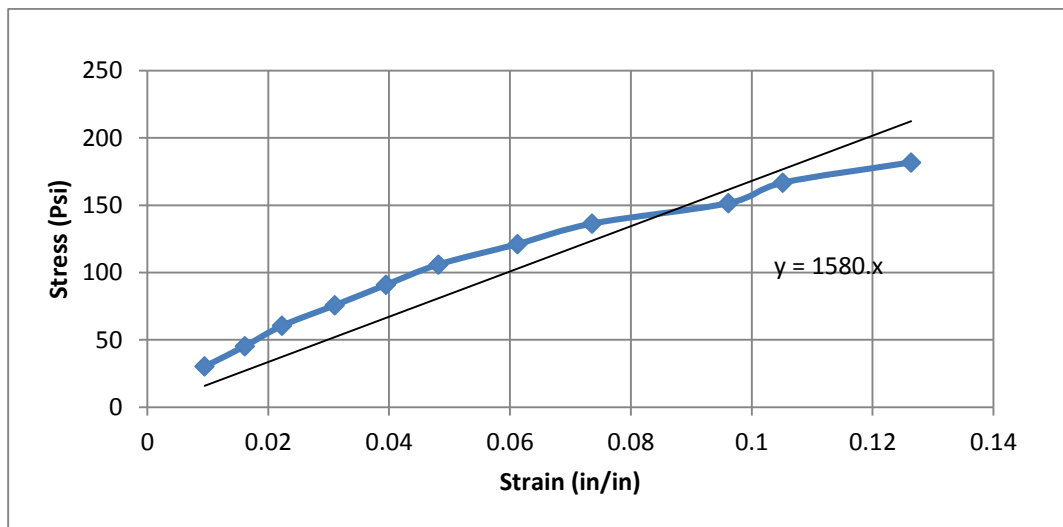


Figure 4-11 - Stress v/s Strain Showing E in CMD =1580 Psi

The above test was repeated four times and the average value was taken as the Young's Modulus in CMD.

Test	Young's Modulus in CMD (Psi)
1	1580
2	1470
3	1490
4	1540
Average	1520

Table 4-5 - Young's Modulus in CMD of Four Different Tests

Thus, the Young's modulus of the orthotropic web in CMD was rounded to 1500 Psi.

The density of the web was also measured by estimating the mass of the web taken in stacks. The volume was calculated using the dimensions of the sample. Multiple stacks of web were taken into account and an average density is found out to be 0.00544 lb/in³.

Orthotropic Web properties (Polypropylene Spun-bond)

The material properties of the orthotropic material are as shown in Table 4-6.

Length, a	Width, b	Thickness, t	E in MD, E _x	E in CMD, E _y	ν_{xy}	G
30"	6"	0.0055"	12000 Psi	1500 Psi	1.8 ²	1030 Psi

Table 4-6 – Material Properties of Orthotropic Web

² Kimberly-Clark Corporation provided the orthotropic web as well as the Poisson's ratio of the web.

CHAPTER V

FINITE ELEMENT MODEL

Finite Element Analysis Using Abaqus

A commercial finite element analysis package (Abaqus 6.14) will be used to model the isotropic and orthotropic webs described in chapter 4. An Abaqus Standard/Explicit model was used to run simulations that were similar to the experimental tests. A 3D deformable part, web of length 30" and width 6" with continuous and homogeneous shell elements (extrusion type) was created. For the isotropic web a uniform material with density 0.00013 and elastic isotropic properties with Young's Modulus 600,000 and Poisson's Ratio 0.35 were assigned to the part created. A section with thickness 0.00048" was created and assigned to the part web. Mesh was generated in the part such that each element size is 0.08" * 0.08". This mesh size was selected to be much smaller than the expected wavelengths during tests and will be shown to be adequate to determine both the trough wavelengths and amplitude. A 4-node, quadrilateral, stress/displacement shell elements with reduced integration were used. The simulation was made to run in three steps using Implicit Dynamic method with a quasi-static assumption. The first step was called as initial step, the second step as velocity and the third one as run. In the initial step the constraints were defined, the time period of second step, velocity was for about 1 second and the third step, run was for about 9 seconds. The left end of the web was totally fixed in all three steps of simulation. The right end of the web was set to move uniformly at an MD velocity = 0.0378 in/s. It was constrained in all other directions. This MD velocity in the web induces uniform web tension, which increases throughout time in the simulation.

The step amplitude created in Abaqus is as shown in Figure 5-1.

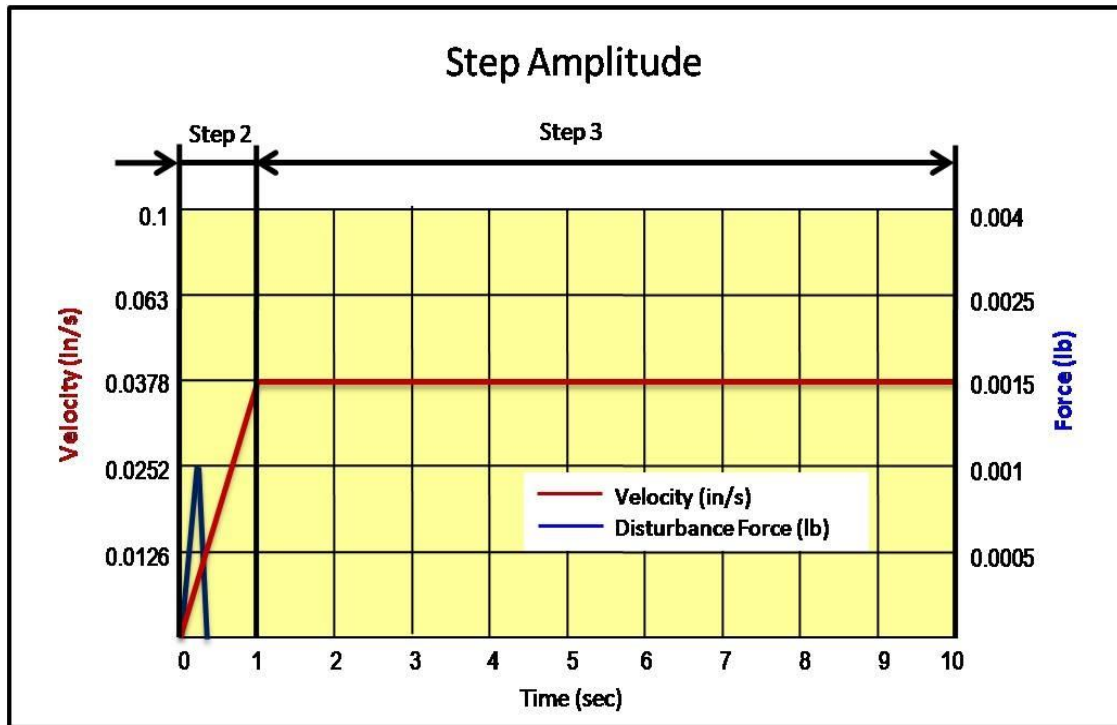


Figure 5-1 - Step Amplitude in Abaqus (Isotropic Web)

To induce buckling in a web with perfect geometry in Abaqus, disturbances are usually applied. A disturbance force = 0.001 lb was applied at the center of the web as shown in Figure 5-2. The disturbance force was set to 0 initially and reaches maximum at 0.3 seconds and vanishes at 0.4 seconds.

Abaqus will provide output at several time steps throughout the simulation. The output provided at these time steps will be used to estimate the wavelength and amplitude at various strains. The out-of-plane displacement was requested as output in the results. At each time step the out-of-plane deformation will be used to produce a mid-span chart of the out-of-plane deformation across the web width. These should be the largest amplitudes and the wavelength will be estimated from these charts.

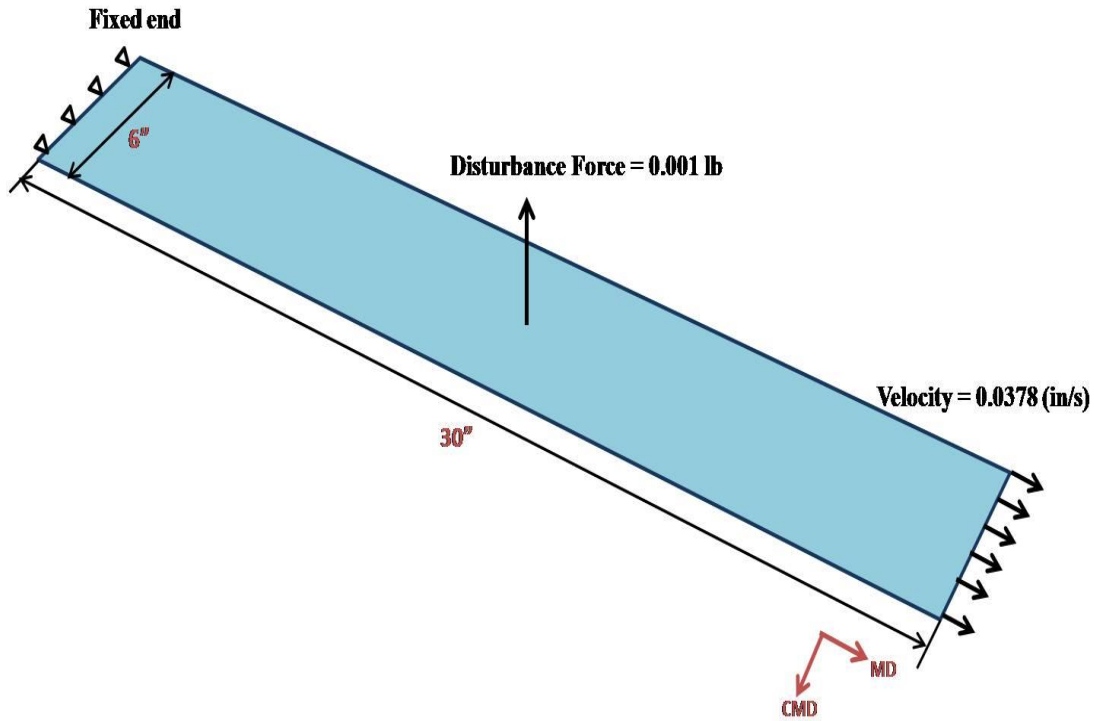


Figure 5-2 - Abaqus Simulation Model

A similar model was created for simulating the troughs formed in the orthotropic web with few changes. A 3D deformable part of length 30” and width 5” with continuous and homogeneous shell elements was created. A uniform material with density 0.00544 and elastic properties with Young’s Modulus in the MD equal to 12000 Psi and the CMD Modulus was set to 1500 Psi. The Poisson’s ratio in MD (V_{xy}) was set to be equal to 1.8 and Abaqus uses Maxwell equation to calculate the Poisson’s ratio in CMD (V_{yx}). A section with thickness 0.0055” is created and assigned to the part web. The disturbance force was set to 0.001 lbs to induce the formation of troughs. The third step time was increased to 14 seconds as shown in Figure 5-3 because for the web boundary moving with a velocity equal to 0.0378 in/sec, a desired load equal to 6 lbs was attained at 13.93 seconds. Again, the output out-of-plane displacement was plotted as a function of width of the web at loads ranging from 2-6 lbs at the mid-span location.

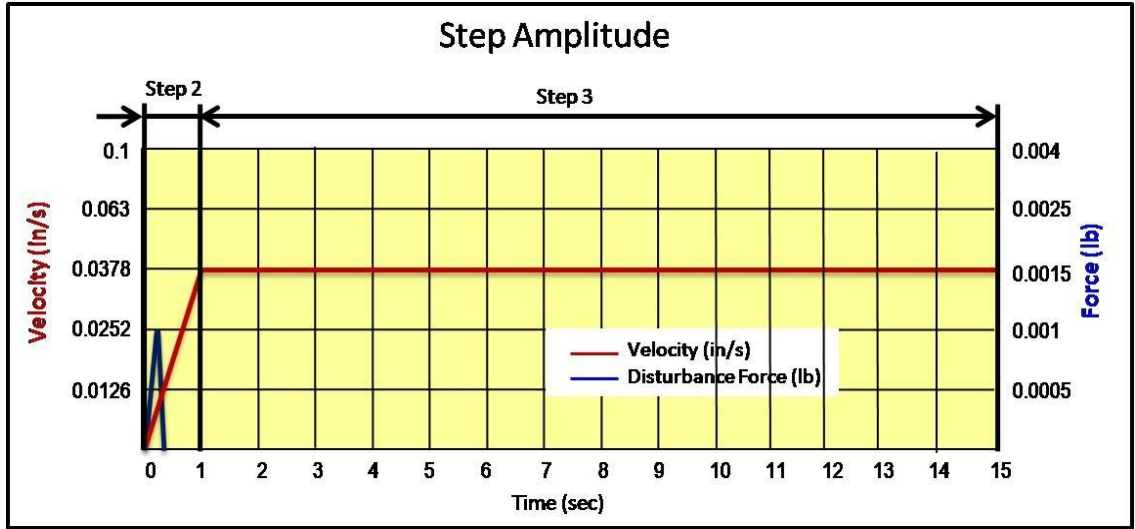


Figure 5-3 - Step Amplitude in Abaqus (Orthotropic Web)

CHAPTER VI

RESULTS AND COMPARISONS

Experimental and Abaqus Results of Isotropic Web

An isotropic web of length 30" and width 6" was tested in the laboratory. The web was subjected to 13 strain levels varying from 0.0012-0.0081. The same experiment was repeated thrice to see the consistency in the profile of troughs formed in the web. The plot of out-of-plane displacement with respect to width at strain levels 0.00289, 0.00463 and 0.00810 are shown in Figures 6-1, 6-2 and 6-3. Additional results for out-of-plane displacement measured at all strain levels are presented in the appendix.

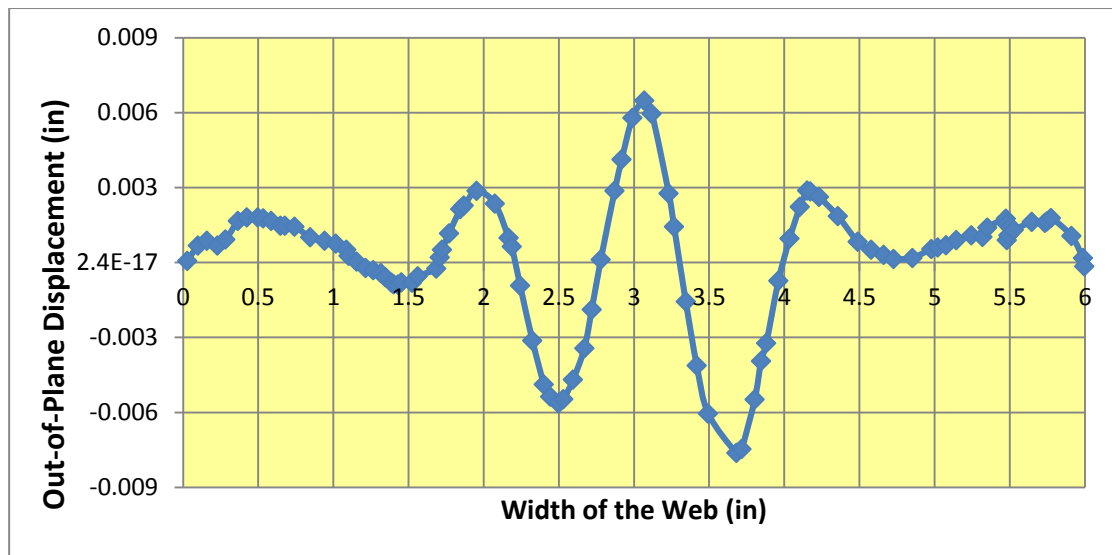


Figure 6-1 - Experimental Results for the Isotropic Web at a Strain Level of 0.00289

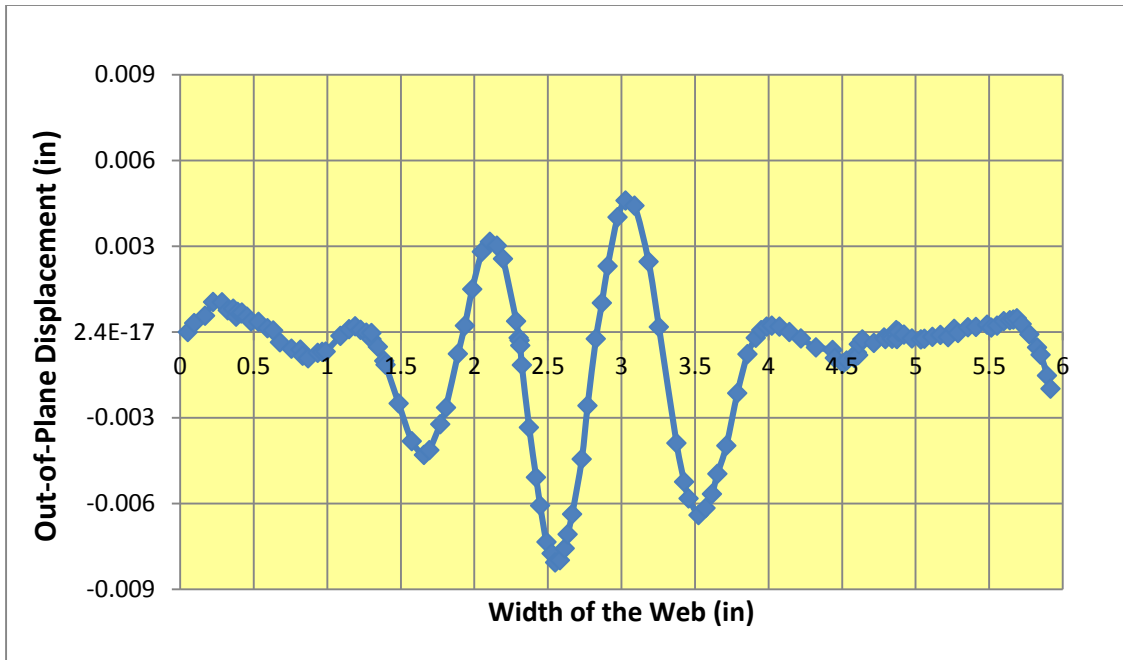


Figure 6-2 - Experimental Results for the Isotropic Web at a Strain Level of 0.00463

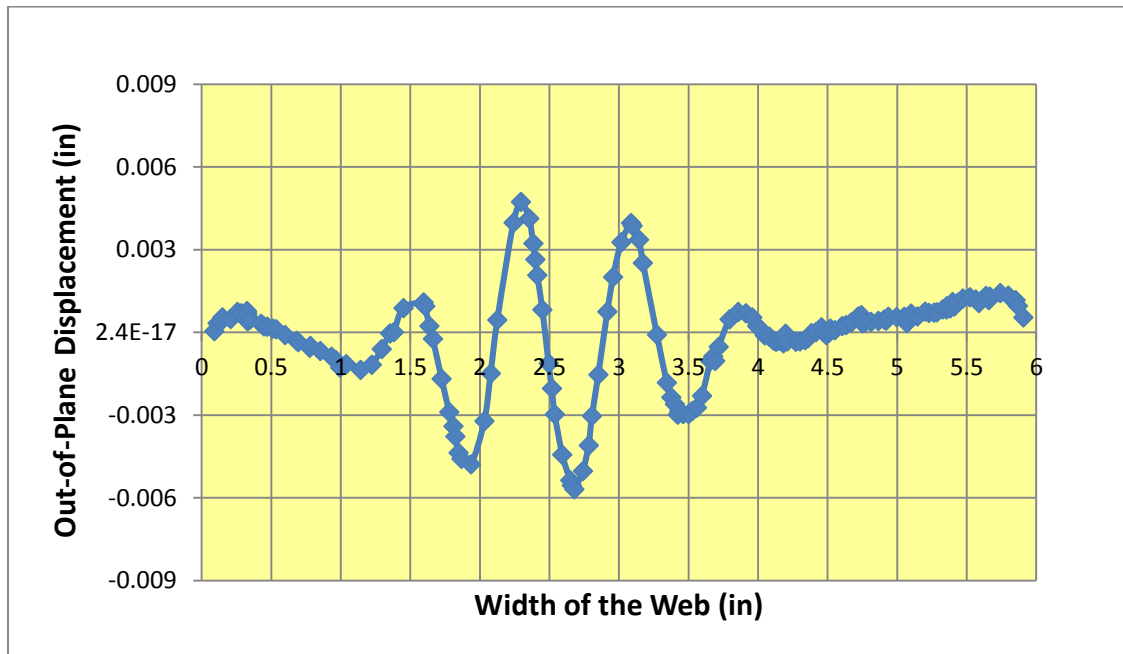


Figure 6-3 - Experimental Results for the Isotropic Web at a Strain Level of 0.0081

To demonstrate the repeatability of these tests, each test was conducted three times and each test was conducted with a new web sample. In Figures 6-4, 6-5 and 6-6 good repeatability is demonstrated for MD strain levels of 0.00289, 0.00463 and 0.0081. At the highest strain level (0.0081) the average MD stress was 4860 Psi which is significantly less than the 12-13 Ksi Dupont Quotes for the yield strength of oriented polyester at room temperature. Thus, little or no elastic deformation occurred during these tests.

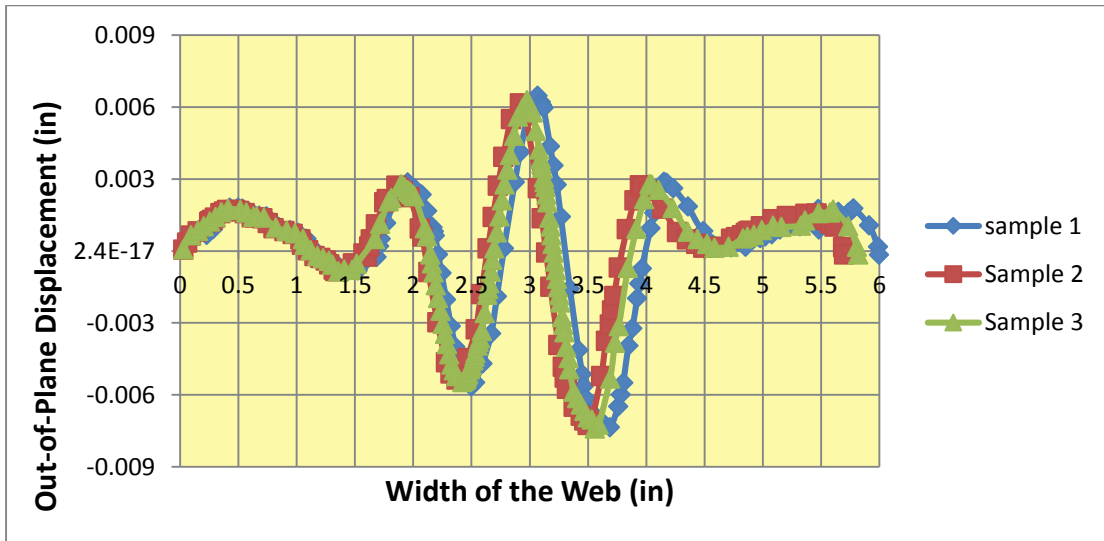


Figure 6-4 - Repeatability Tests for Troughs in Isotropic Web at a Strain Level of 0.00289

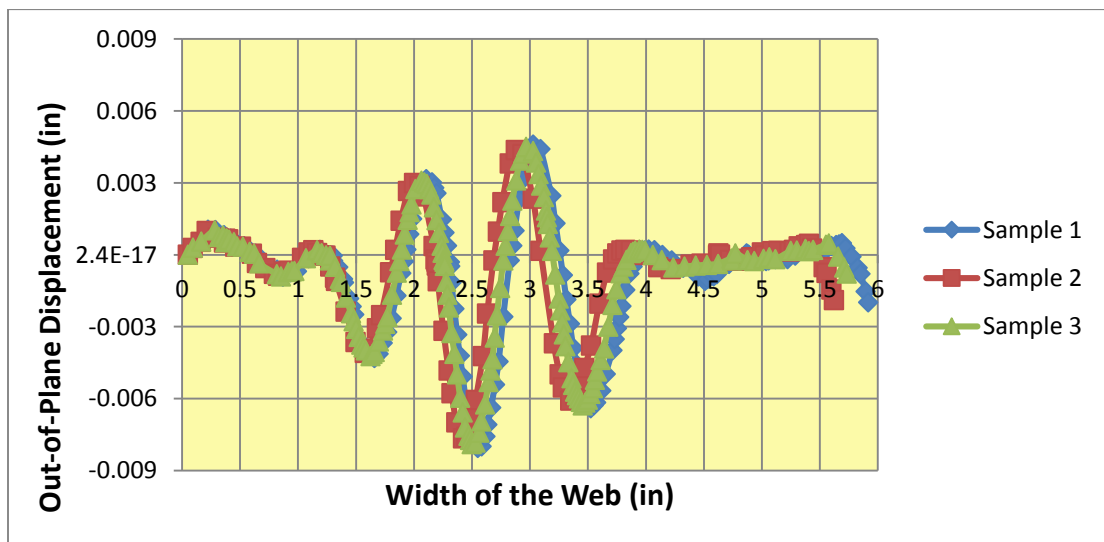


Figure 6-5 - Repeatability Tests for Troughs in Isotropic Web at a Strain Level of 0.00463

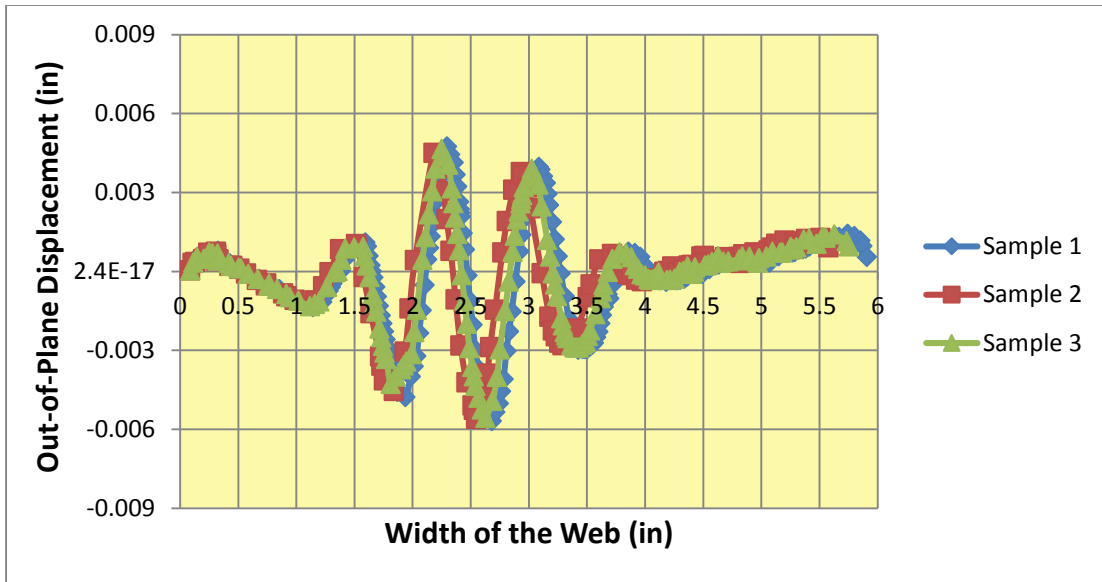


Figure 6-6 - Repeatability Tests for Troughs in Isotropic Web at a Strain Level of 0.0081

Figure 6-7 shows how the wavelength and amplitude is estimated from the excel spreadsheet.

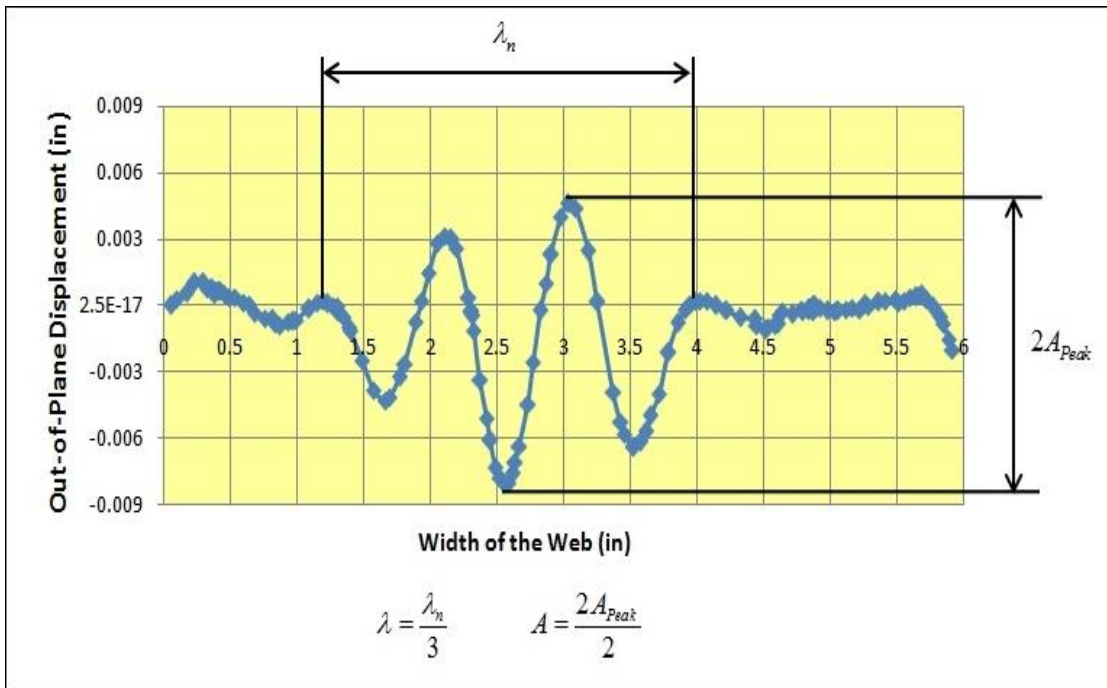


Figure 6-7 - Depicting the Estimation of Wavelength and Amplitude (Experiment Results)

Tables 6-1 and 6-2 shows the wavelength and amplitude of troughs estimated from test data on three different samples of web. The average and error is calculated using an excel spreadsheet.

Experimental Results of Wavelength (in)					
Strain	Sample 1	Sample 2	Sample 3	Average	Error
0.0012	1.27	1.23	1.25	1.25	0.01
0.0017	1.23	1.20	1.21	1.22	0.01
0.0023	1.19	1.16	1.18	1.17	0.01
0.0029	1.18	1.12	1.14	1.15	0.01
0.0035	1.07	1.02	1.05	1.04	0.01
0.0041	0.99	0.94	0.96	0.96	0.01
0.0046	0.97	0.92	0.95	0.95	0.01
0.0052	0.95	0.90	0.92	0.92	0.01
0.0058	0.92	0.87	0.90	0.90	0.01
0.0064	0.89	0.84	0.85	0.86	0.01
0.0069	0.85	0.81	0.78	0.81	0.01
0.0075	0.79	0.75	0.75	0.76	0.01
0.0081	0.78	0.70	0.72	0.73	0.02

Table 6-1 - Experimental Results of Wavelength on the Isotropic Web (in)

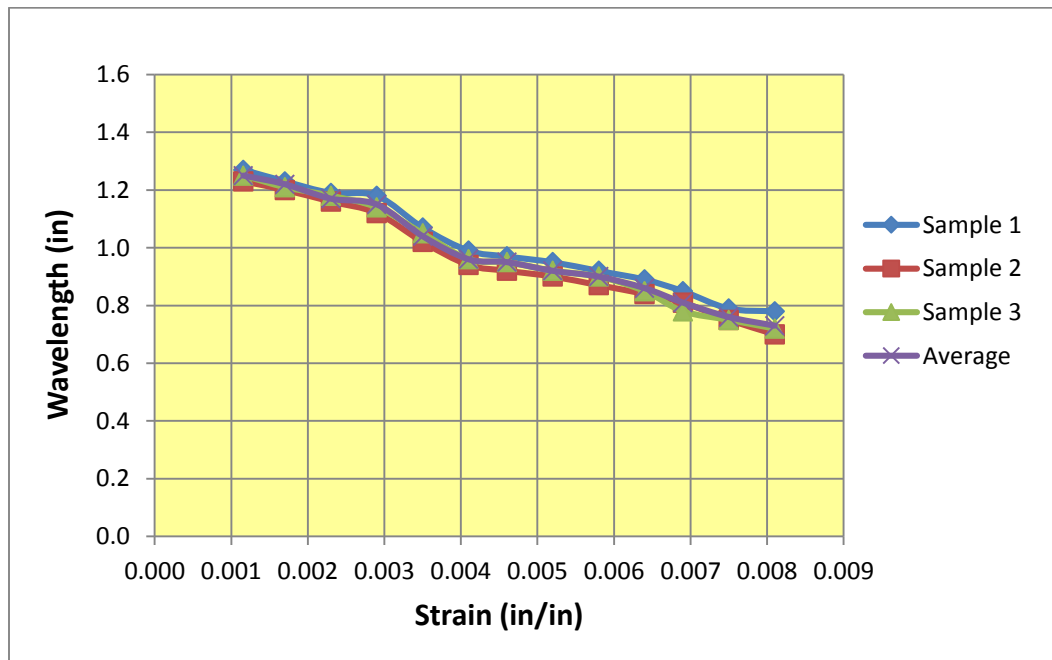


Figure 6-8 - Experimental Results of Wavelength on the Isotropic Web (in)

Experimental Results of Amplitude (in)					
Strain (in/in)	Sample 1	Sample 2	Sample 3	Average	Error
0.0012	0.0112	0.0104	0.0107	0.0108	0.0001
0.0017	0.0093	0.0091	0.0092	0.0092	0.0001
0.0023	0.0083	0.0081	0.0082	0.0082	0.0001
0.0029	0.0071	0.0067	0.0068	0.0069	0.0001
0.0035	0.0065	0.0061	0.0063	0.0063	0.0001
0.0041	0.0064	0.0061	0.0062	0.0062	0.0001
0.0046	0.0063	0.0059	0.0060	0.0061	0.0001
0.0052	0.0060	0.0057	0.0058	0.0058	0.0001
0.0058	0.0059	0.0056	0.0056	0.0057	0.0001
0.0064	0.0054	0.0053	0.0053	0.0053	0.0000
0.0069	0.0053	0.0051	0.0052	0.0052	0.0001
0.0075	0.0050	0.0051	0.0051	0.0051	0.0000
0.0081	0.0048	0.0047	0.0047	0.0047	0.0000

Table 6-2 - Experimental Results of Amplitude on the Isotropic Web (in)

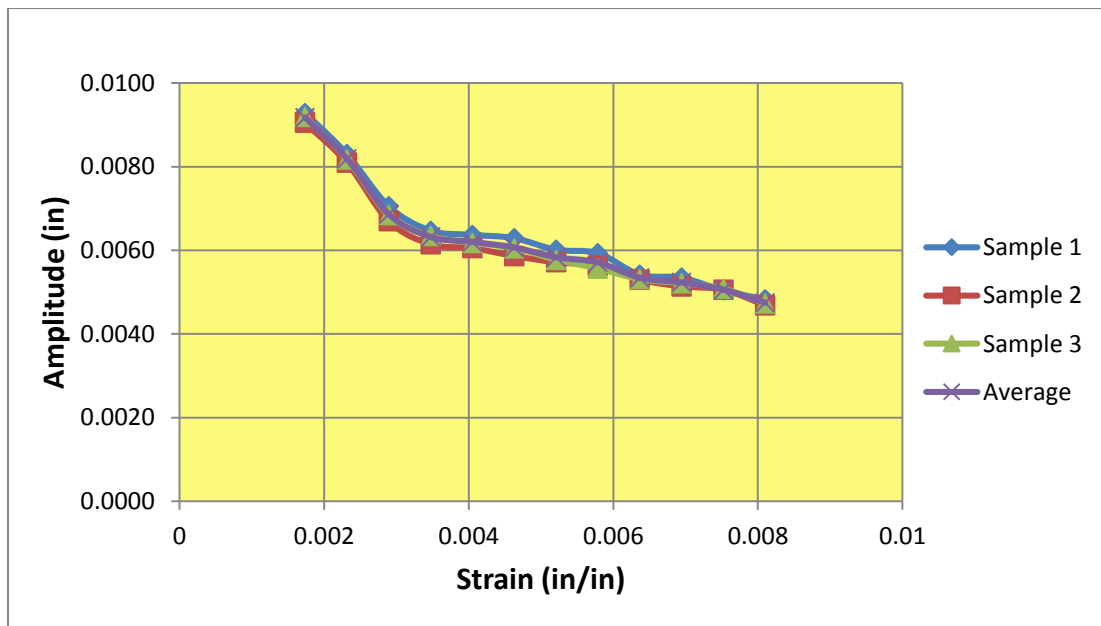


Figure 6-9 - Experiment Results of Amplitude on the Isotropic Web (in)

Finite Element Analysis (Abaqus) Results

Finite element analysis simulation was made to run for an isotropic web model discussed earlier. The Wavelength and Amplitude are calculated by measuring the out-of-plane displacement of web at various strains as shown in Figure 6-10.

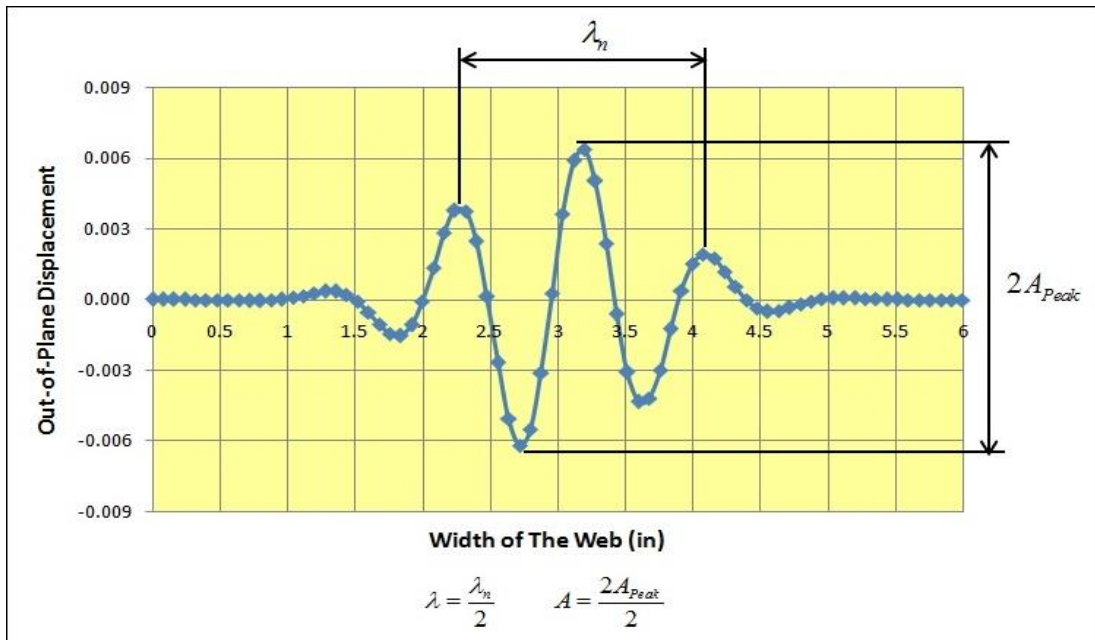


Figure 6-10 - Depicting the Estimation of Wavelength and Amplitude (Abaqus Results)

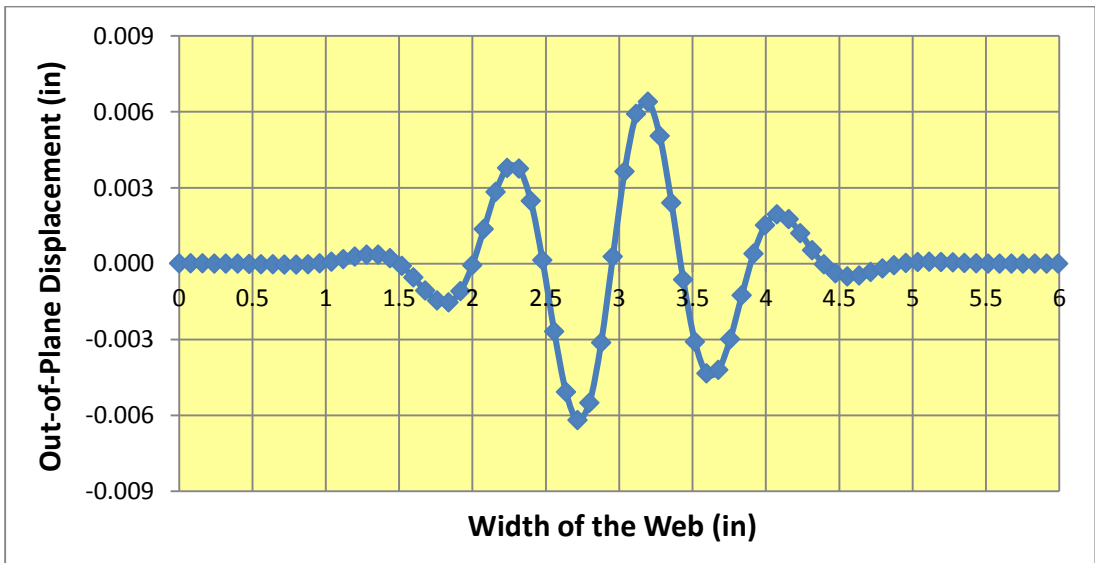


Figure 6-11 - Abaqus Results for the Isotropic Web at a Strain Level of 0.00281

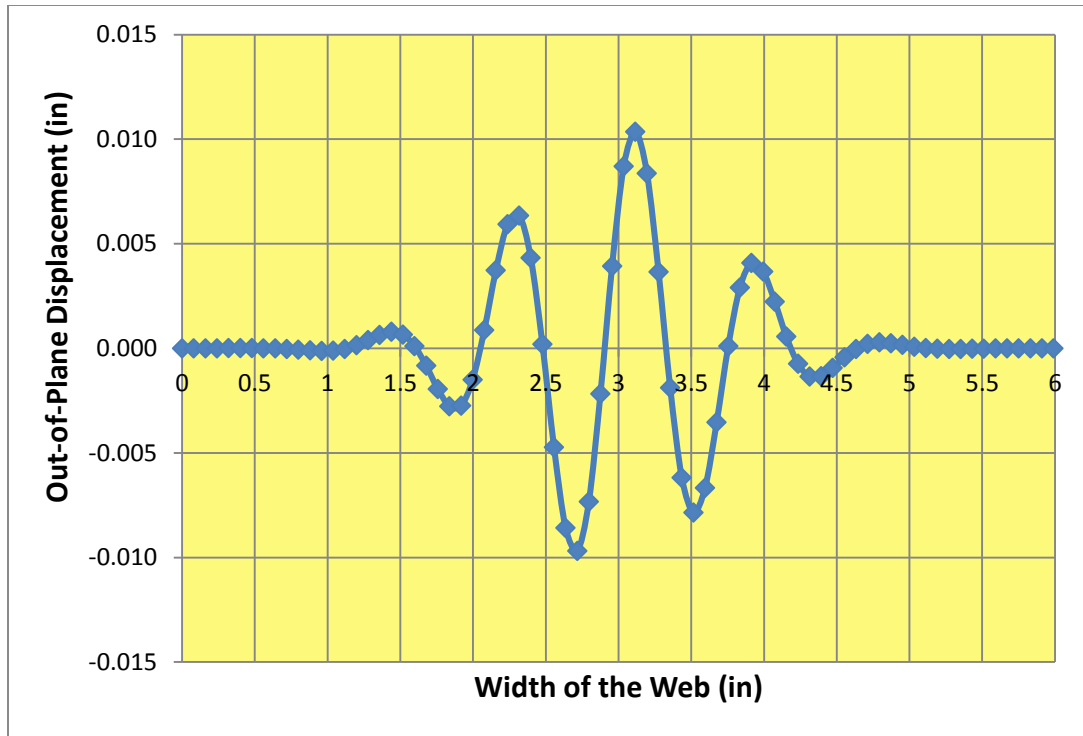


Figure 6-12 - Abaqus Results for the Isotropic Web at a Strain Level of 0.00463

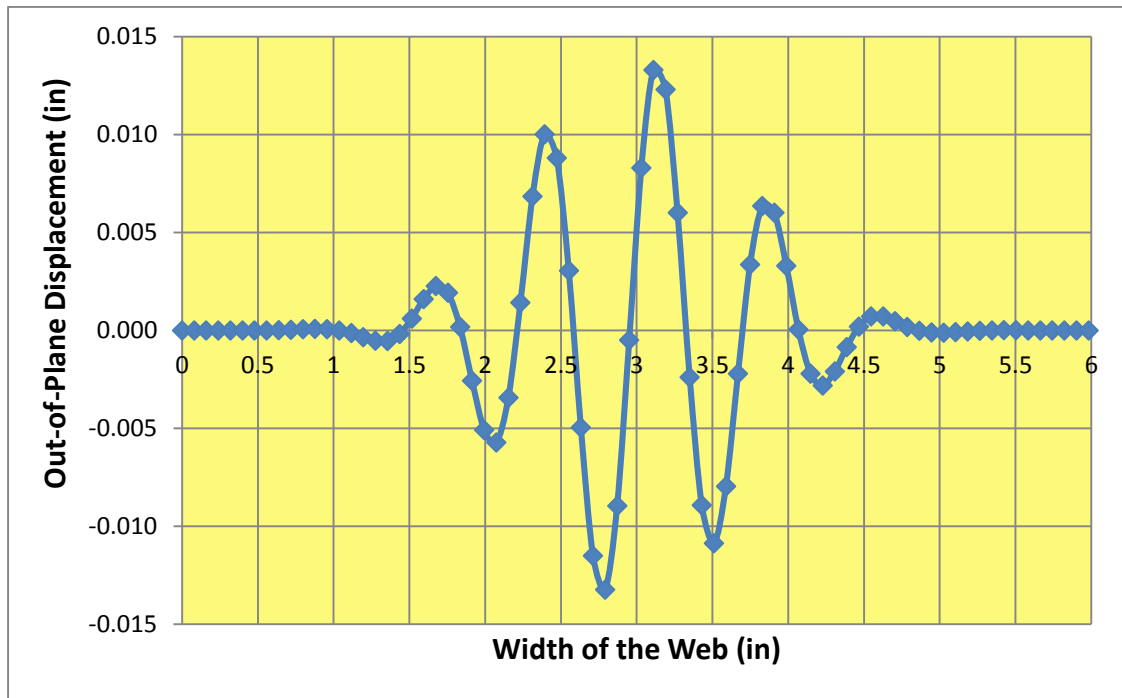


Figure 6-13 - Abaqus Results for the Isotropic Web at a Strain Level of 0.0081

Comparison of Experimental and Finite Element Analysis Results with Theoretical Results of an Isotropic Web

The wavelength of troughs formed on isotropic web is calculated using the formulae derived by Cerda (38) and Dr. Good (8). Both these equations are quite similar. The agreement between test, finite element analysis and equations (8) and (38) are quite good.

Comparison of Wavelength (in)			
Strain	Experiment	Abaqus	Good (8)
0.0012	1.25	1.24	1.28
0.0017	1.21	1.01	1.16
0.0023	1.17	0.96	1.08
0.0029	1.11	0.93	1.02
0.0035	1.04	0.88	0.97
0.0041	0.96	0.84	0.94
0.0046	0.95	0.80	0.91
0.0052	0.92	0.80	0.88
0.0058	0.90	0.80	0.86
0.0064	0.86	0.76	0.84
0.0069	0.81	0.76	0.82
0.0075	0.76	0.76	0.80
0.0081	0.73	0.72	0.79

Table 6-3 - Comparison of Wavelength with Theoretical Results on the Isotropic Web

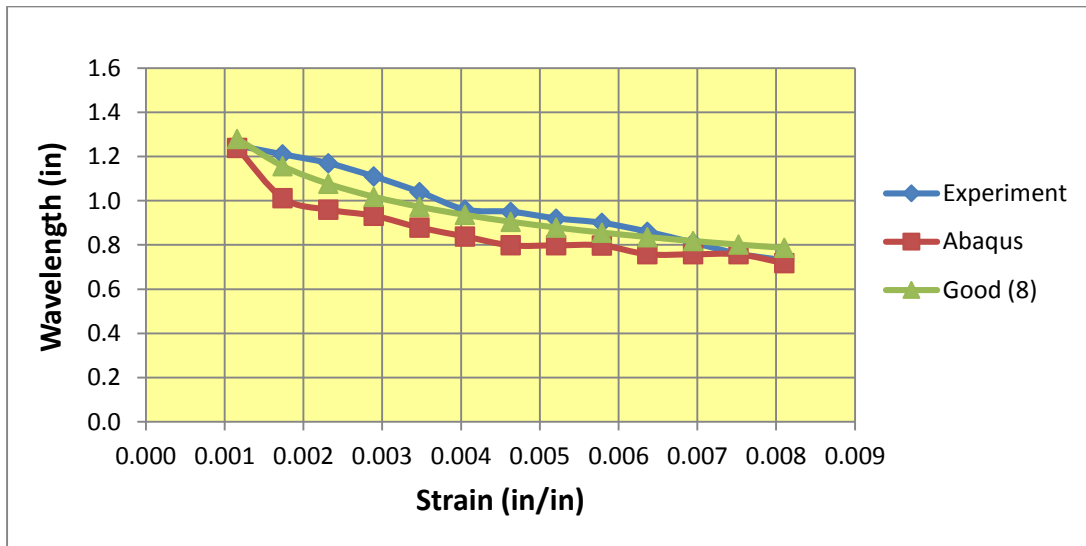


Figure 6-14 - Comparison of Wavelength with Theoretical Results on the Isotropic Web

The amplitude of troughs formed on isotropic web is calculated using the formulae derived by Cerda (39) and Dr. Good (44) and compared with the finite element simulations and test results in Table 6-4 and Figure 6-15.

Comparison of Amplitude (in)				
Strain	Experiment	Abaqus	Good (44)	Cerda (39)
0.0012	0.0108	0.0000	0.00820	0.0116
0.0017	0.0092	0.0023	0.00908	0.0128
0.0023	0.0082	0.0047	0.00975	0.0138
0.0029	0.0068	0.0064	0.01031	0.0146
0.0035	0.0063	0.0079	0.01079	0.0153
0.0041	0.0062	0.0092	0.01122	0.0159
0.0046	0.0060	0.0104	0.01160	0.0164
0.0052	0.0058	0.0110	0.01195	0.0169
0.0058	0.0057	0.0118	0.01227	0.0173
0.0064	0.0053	0.0122	0.01256	0.0178
0.0069	0.0052	0.0126	0.01284	0.0182
0.0075	0.0050	0.0129	0.01310	0.0185
0.0081	0.0047	0.0133	0.01334	0.0189

Table 6-4 - Comparison of Amplitude with Theoretical Results on the Isotropic web

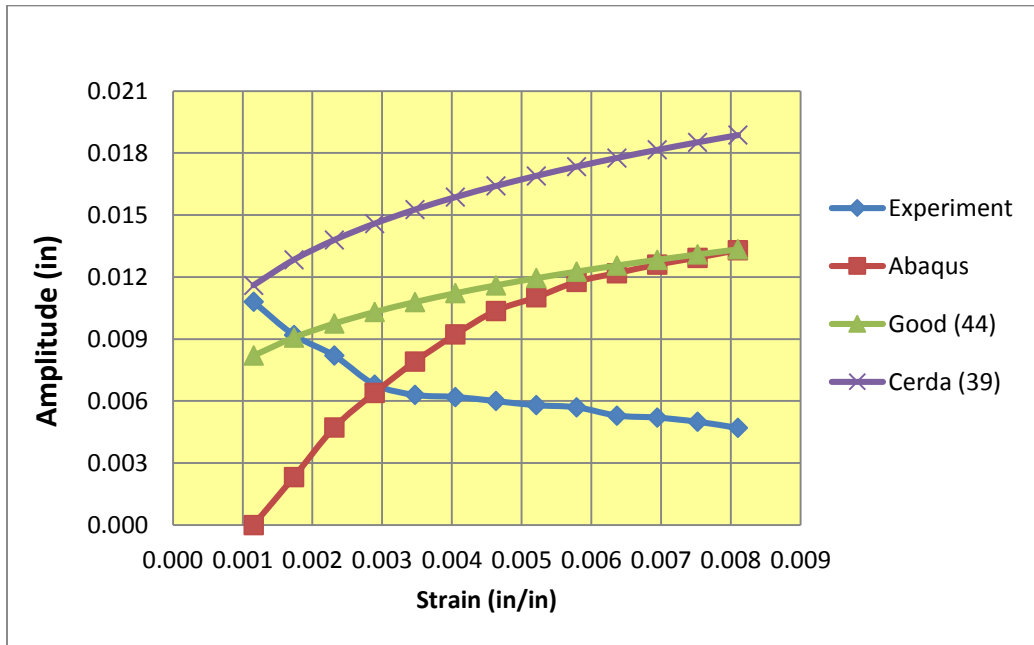


Figure 6-15 - Comparison of Amplitude with Theoretical Results on the Isotropic Web

Theoretically, there should be no buckling below a critical MD strain level, where the critical buckling stress is greater (more negative) than the CMD compressive stresses. At an MD strain 0.0012 (in/in), the critical buckling stress is estimated to be equal to -0.64 Psi. At the same strain level, the CMD compressive stresses from Abaqus are as shown in Figure 6-16.

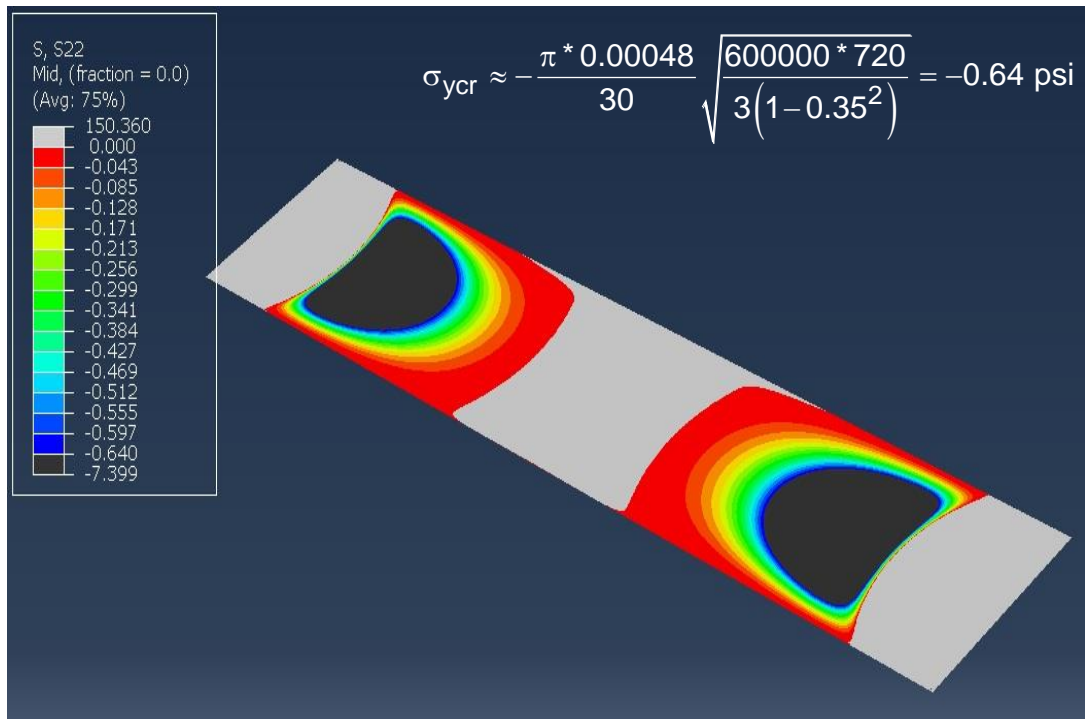


Figure 6-16 – CMD Compressive Stresses at a MD Strain level of 0.0012 (in/in)

From Figure 6-16, it can be seen that CMD compressive stresses are not throughout the span of the web. However, at some locations the CMD compressive stresses are greater than (more negative) than the critical buckling stress. These CMD compressive stresses are not enough to buckle the web at MD strain level of 0.0012.

In contrast to Abaqus results, Good (44) and Cerda (39) derived from the theory of inextensibility predict trough amplitudes all the down to zero strain. This shows a shortcoming of these expressions. At MD strains 0 to 0.0012 the strains produced by Poisson contraction are producing extensible strains and not out-of-plane deformation.

In contrast to Abaqus and theoretical results, the experimental result of troughs amplitude decrease with increase in MD strain. This is very different from the result of troughs amplitude from Abaqus, Cerda (39) and Good (44) increase with increase in MD strain. This is the result of clamping the web and this behavior is also witnessed by Zheng [10] as shown in Figure 6-17.

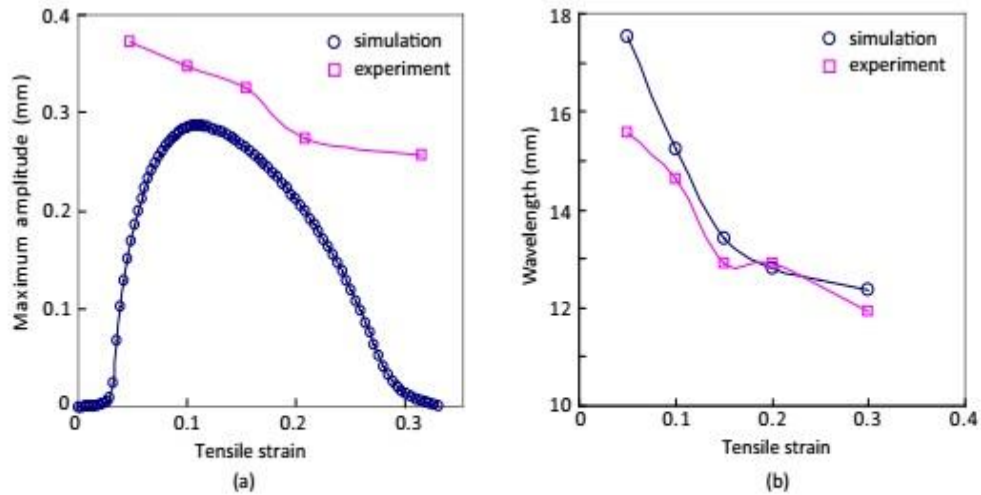


Figure 5.3: Comparison of the experimental and numerical results for (a) the maximum wrinkle amplitude, and (b) the wavelength of the largest wrinkle, of the 254 × 101.6 mm (10 × 4 inch) membrane vs. tensile strain.

Figure 6-17 – Image from Zheng [10] showing Amplitude Results

From Figure 6-15, Good’s equation (44) and Abaqus produce amplitude results that agree well for MD strains ranging from 0.003 to 0.008 that envelop the experiment amplitudes. Thus, Good’s equation (44) has an MD strain range over which it is a useful predictor.

Experimental and Abaqus Results of Orthotropic Web

The orthotropic web of length 30” and width 5” was tested for out-of-plane displacement in the laboratory. The web was subjected to 5 strain levels varying from 0.006-0.018. The same experiment was repeated thrice with different samples of web to see the consistency in the profile of troughs formed in the web.

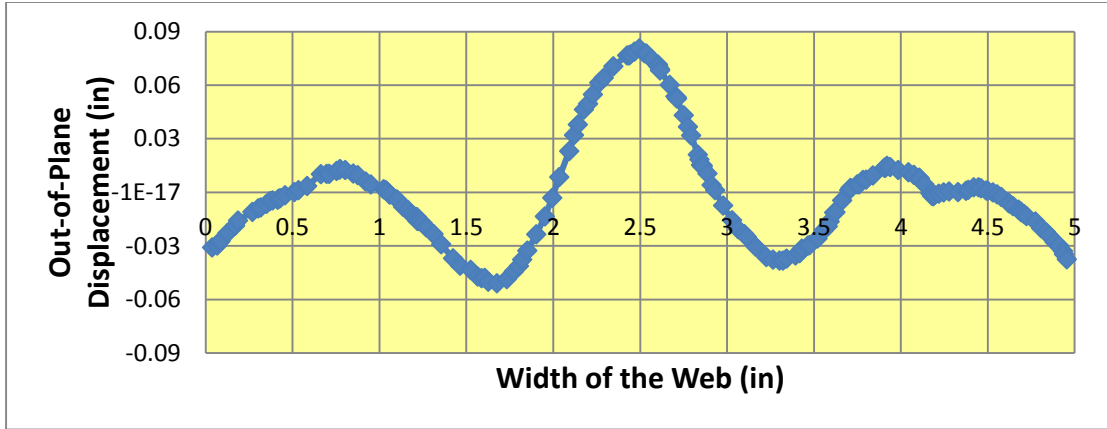


Figure 6-18 - Experimental Results for the Orthotropic Web at a Strain Level of 0.006

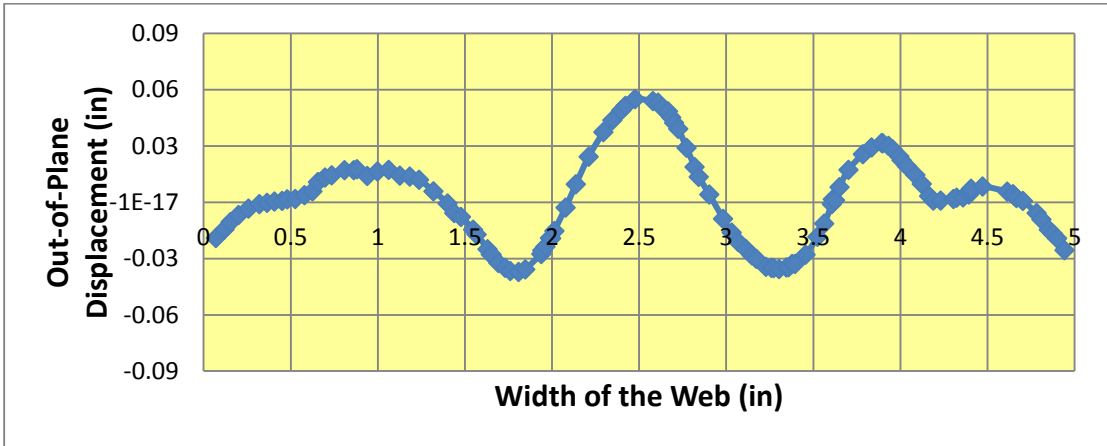


Figure 6-19 - Experimental Results for the Orthotropic Web at a Strain Level of 0.012

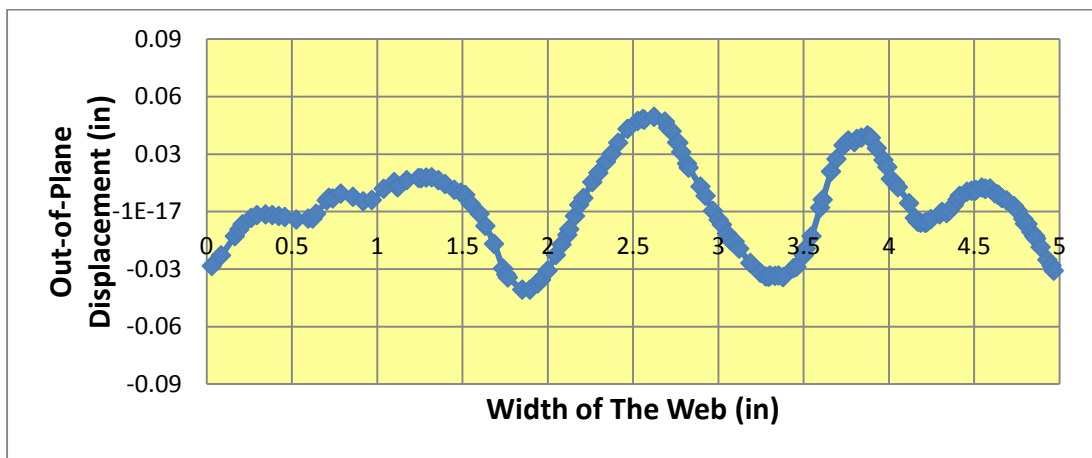


Figure 6-20 - Experimental Results for the orthotropic Web at a Strain Level of 0.018

The profile of troughs formed on different samples of orthotropic web are plotted to check the consistency.

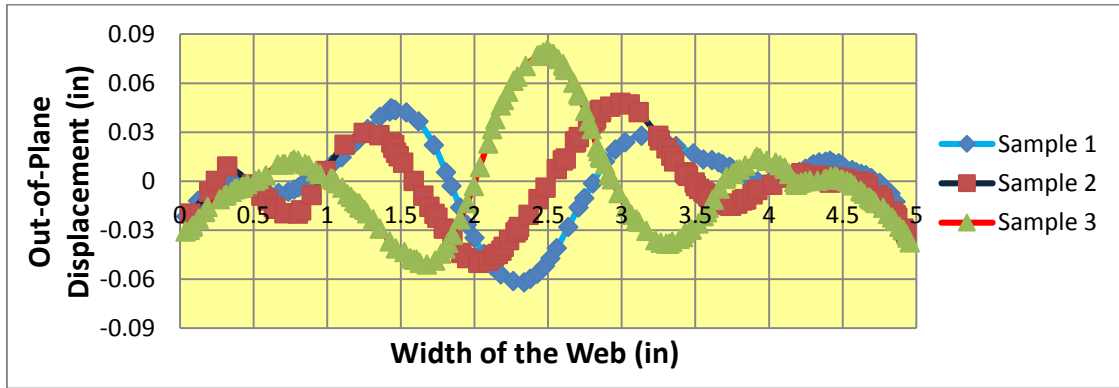


Figure 6-21 - Repeatability Tests for Troughs in Orthotropic Web at a Strain Level of 0.006

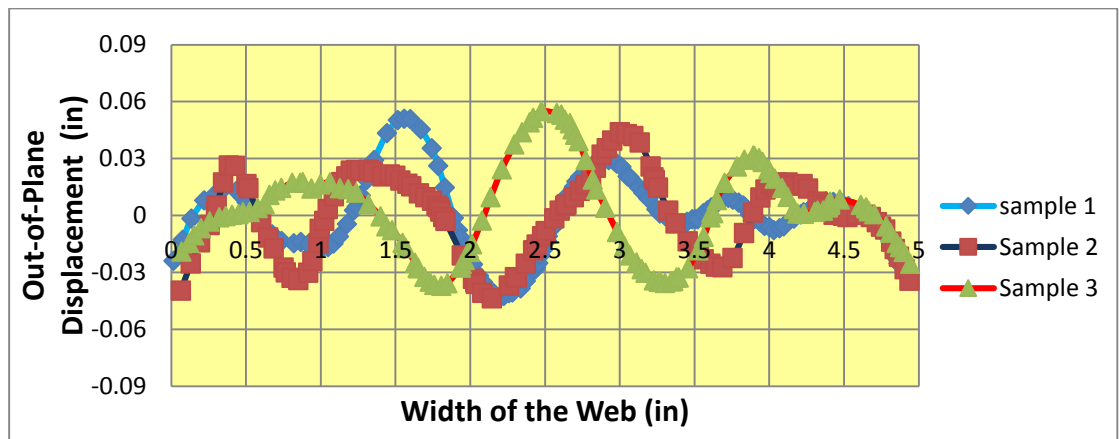


Figure 6-22 - Repeatability Tests for Troughs in Orthotropic Web at a Strain Level of 0.012

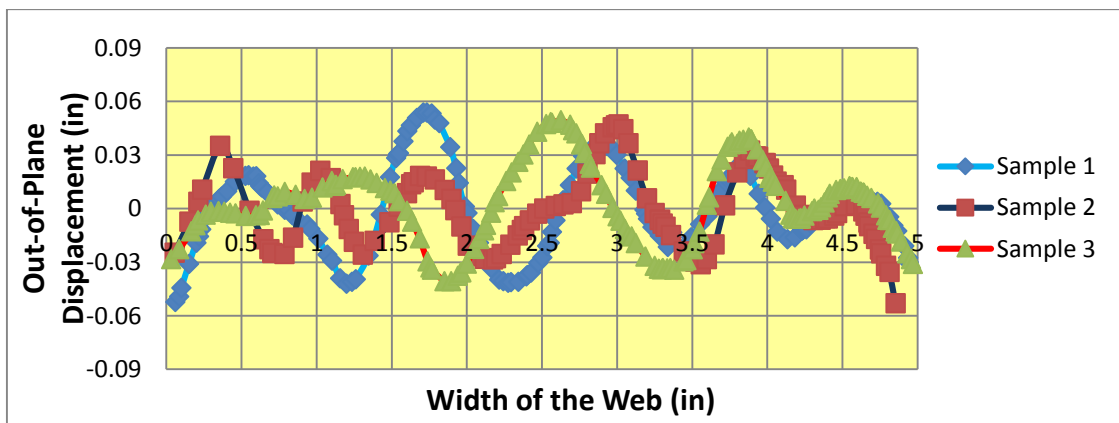


Figure 6-23 - Repeatability Tests for Troughs in Orthotropic Web at a Strain Level of 0.018

From the Figures 6-21, 6-22 and 6-23 it is clear that the profile of troughs formed on different samples of orthotropic web are not as consistent as they were shown to be for the isotropic web in Figures 6-4, 6-5 and 6-6.

Figure 6-24 shows how the wavelength and amplitude is estimated from the excel spreadsheet. Tables 6-5 and 6-6 show the wavelength and amplitude of troughs formed on three different samples of web. Figures 6-25 and 6-26 show how the wavelength and amplitude behave as a function of MD strain level.

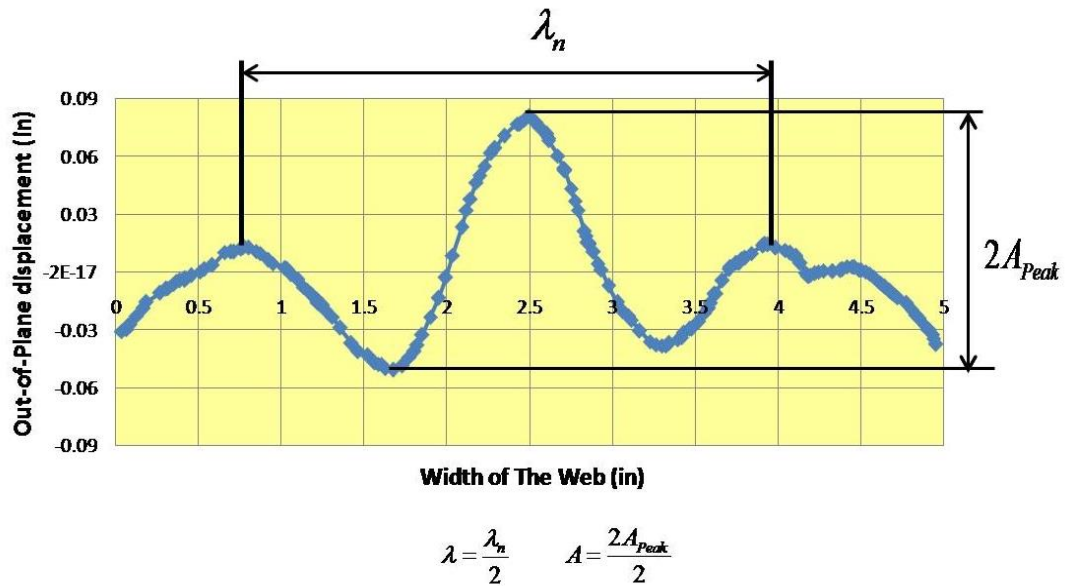


Figure 6-24 - Depicting the Estimation of Wavelength and Amplitude (Experiment Results)

Comparison of Wavelength (in)					
Strain	Sample 1	Sample 2	Sample 3	Average	Error
0.006	1.68	1.74	1.64	1.69	0.027
0.009	1.62	1.68	1.54	1.61	0.040
0.012	1.50	1.54	1.49	1.51	0.013
0.015	1.40	1.46	1.39	1.42	0.020
0.018	1.35	1.38	1.25	1.33	0.040

Table 6-5 - Experimental Results of Wavelength on the Orthotropic Web

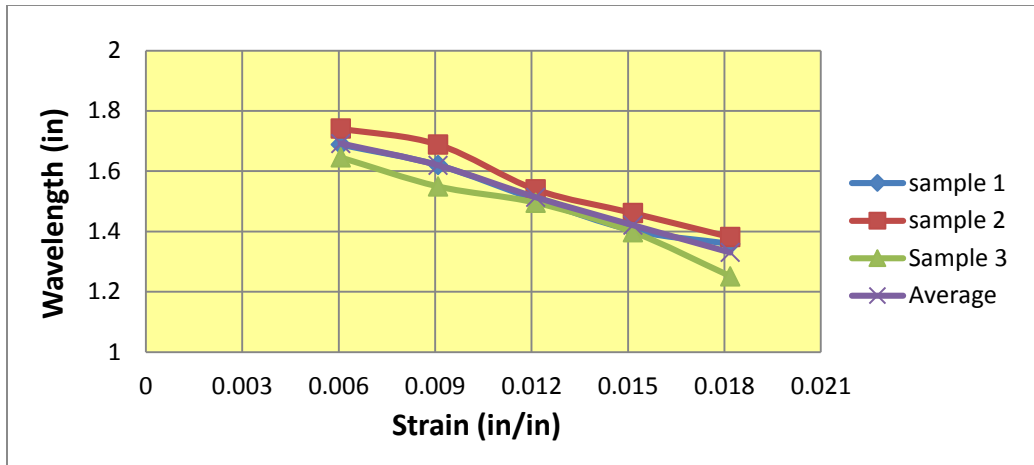


Figure 6-25 - Experimental Results of Wavelength on the Orthotropic Web

Experiment Results of Amplitude on Orthotropic Web (in)					
Strain	Sample 1	Sample 2	Sample 3	Average	Error
0.006	0.053	0.049	0.059	0.053	0.003
0.009	0.047	0.045	0.055	0.049	0.003
0.012	0.046	0.043	0.046	0.045	0.001
0.015	0.047	0.037	0.045	0.043	0.003
0.018	0.047	0.039	0.045	0.043	0.002

Table 6-6 - Experimental Results of Amplitude on the Orthotropic Web

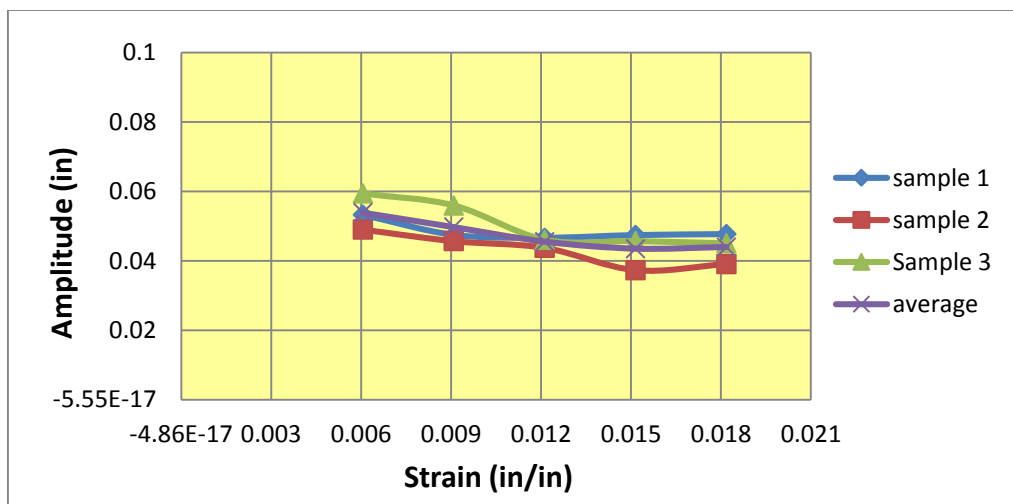


Figure 6-26 - Experimental Results of Amplitude on the Orthotropic Web

Finite Element Analysis (Abaqus) Results

Finite Element Analysis simulation was made to run with material properties of material that we tested in laboratory. Abaqus results show that there is no buckling in the web, even though experimental results show that the troughs are formed when the web is subjected to tension.

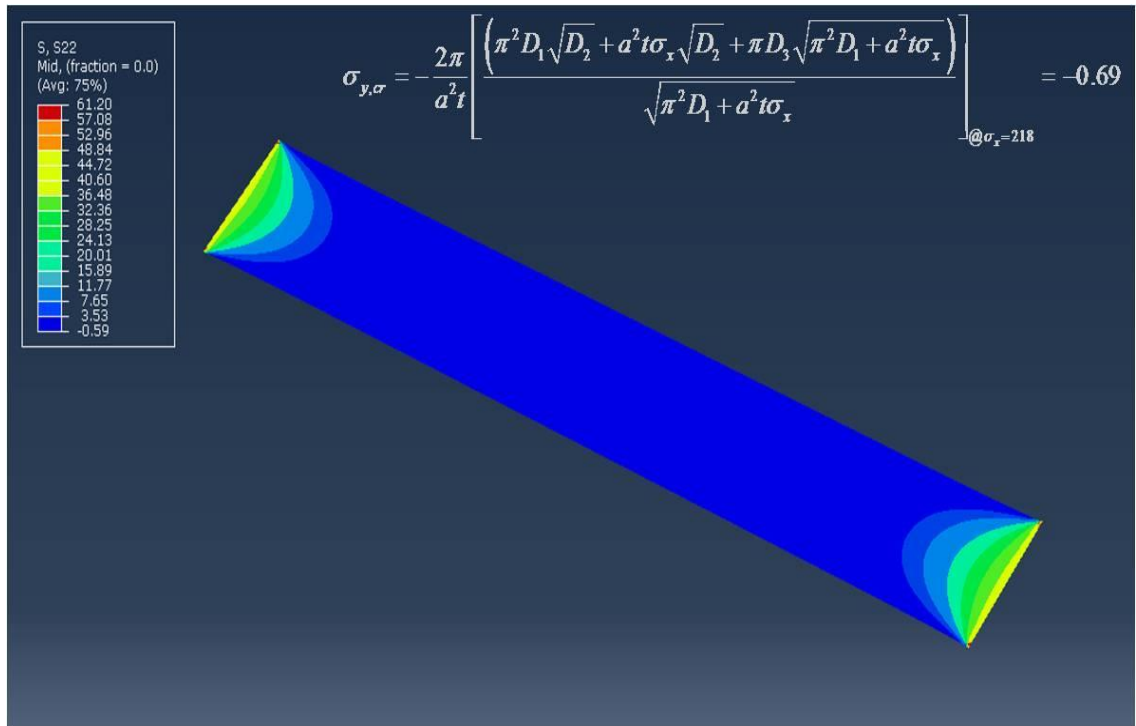


Figure 6-27 - CMD Compressive Stresses at a MD Strain level of 0.018

From Figure 6-27, the CMD compressive stress at MD strain level of 0.018 is -0.59 Psi. From equation (15), the critical compressive stress is estimated to be -0.69 Psi. Since, the critical compressive stress is greater (more negative) than the CMD compressive stress, the web did not buckle.

Explanation

From the above results it is clear that the orthotropic web doesn't buckle in Abaqus but the experimental results shows that the web buckled at low strains. It is believed the web buckled

because of non-uniformity of the web which we haven't defined in Abaqus model. To prove this claim a picture was taken in the lab to show the non-uniformity of the web.

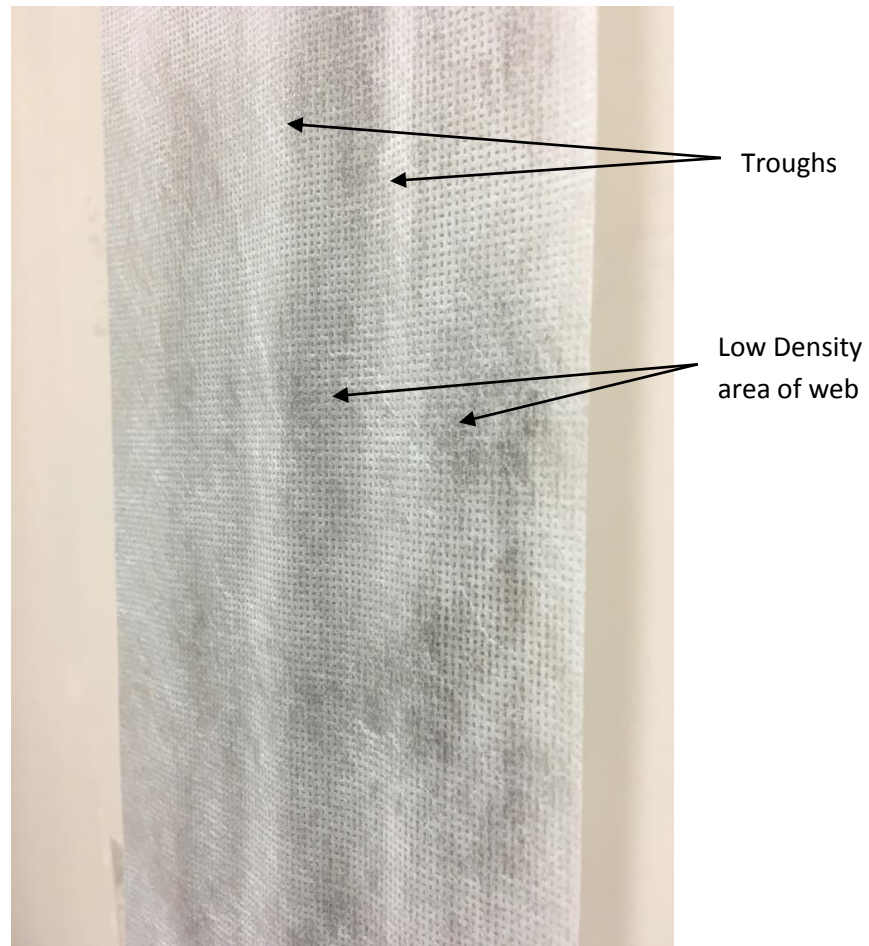


Figure 6-28 - Picture Depicting Non-Uniform Thickness in the Orthotropic Web

In the above image, the darker areas are of less thickness or low density area compared to the other areas in the web. It was observed that when troughs are formed in the web due to stress the amplitude is maximum at low density area of web. To prove this claim we measured the out-of-plane displacement of the same web shown in the image above. Also, the formation of troughs is not continuous across the length of the web. The test out-of-plane displacement is plotted over the web width in Figure 6-28.

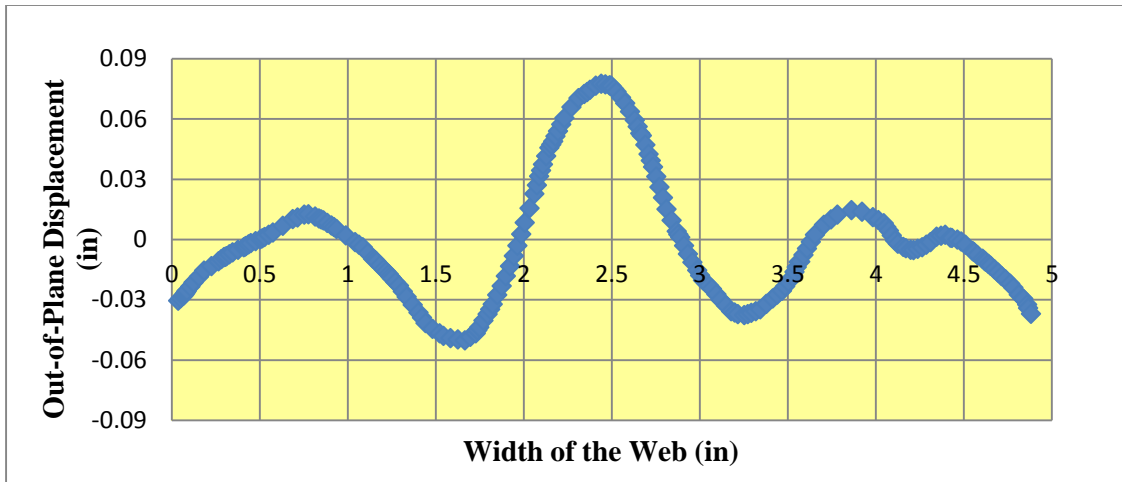


Figure 6-29 - Out-of-plane Displacement Associated with the Web Shown in Figure 6-28

From the Figure 6-29, it appears that the web buckles coincide with the density variation seen in Figure 6-28. The small out-of-plane displacement formed between 4 and 4.5 inches of the web width is due to the low area density of the web shown in Figure 6-28.

Comparison of Experiment Results with Theoretical Results on Orthotropic Web

As Finite Element Analysis simulation results did not show any signs of buckling. The experimental results of wavelength are compared with that of theoretical results calculated using the formulae given by equation (18).

Comparison of Wavelength (in)		
Strain	Experiment	Good (18)
0.006	1.69	1.87
0.009	1.61	1.69
0.012	1.51	1.57
0.015	1.42	1.49
0.018	1.33	1.42

Table 6-7 - Comparison of Experimental and Theoretical Wavelength on Orthotropic Web

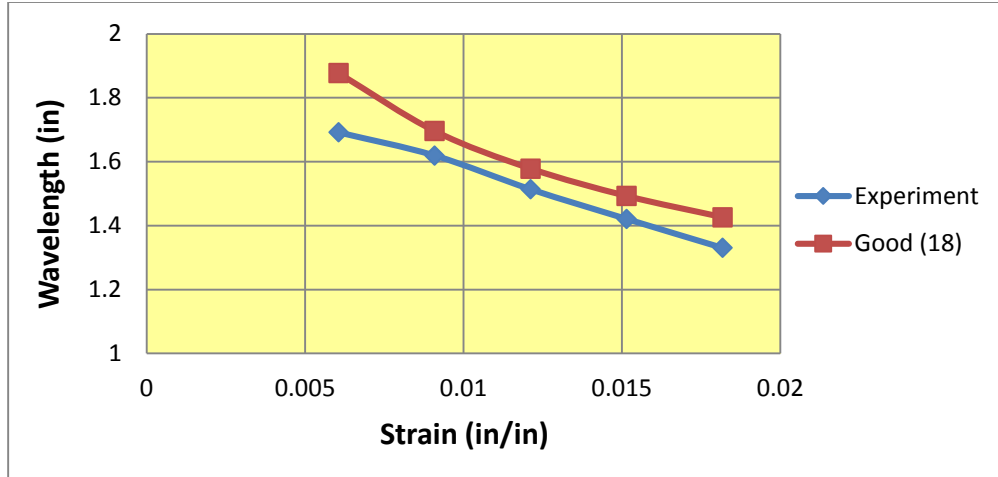


Figure 6-30 - Comparison of Experiment and Theoretical Wavelength on Orthotropic Web

The experimental results of wavelength are compared with that of theoretical results calculated using the formulae given by equation (52).

Comparison of Amplitude (in)		
Stress	Experiment	Nukala (52)
0.006	0.053	0.062
0.009	0.049	0.069
0.012	0.045	0.074
0.015	0.043	0.078
0.018	0.043	0.082

Table 6-8 - Comparison of Experiment and Theoretical Amplitude on Orthotropic Web

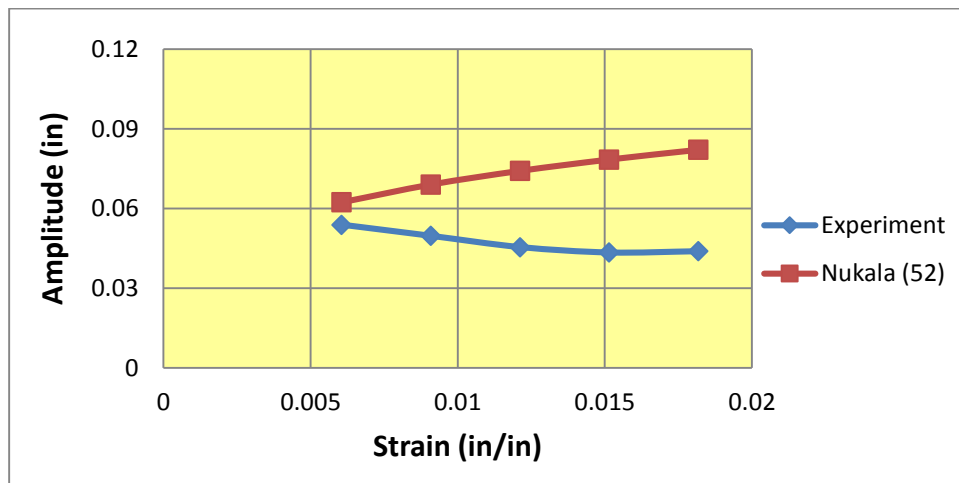


Figure 6-31 - Comparison of Experiment and Theoretical Amplitude on Orthotropic Web

Even though the troughs in the orthotropic web tested did not form as a result of the CMD compressive stresses that formed due to the clamped boundaries and the MD strain equation (18) still provided results that compared nicely with the experiment results in Figure 6-30. Equation (52) enveloped the trough amplitudes witnessed in tests in Figure 6-31.

A Second Orthotropic Example

To test the orthotropic expressions for wavelength (18) and amplitude (52), additional cases were simulated using Abaqus. In these cases the web thickness from the isotropic case were used, the MD modulus of 600,000 Psi was retained but the CMD modulus was decreased to 300,000 Psi.

The complete material properties are listed in Table 6-9.

Length, a	Width, b	Thickness, t	E in MD	E in CMD	ν_{xy}	G
30	6	0.00048	600000	300000	0.3	200000

Table 6-9 – Material Properties of a Pseudo Material

The Wavelength and Amplitude are calculated from Abaqus results as depicted in Figure 6-32.

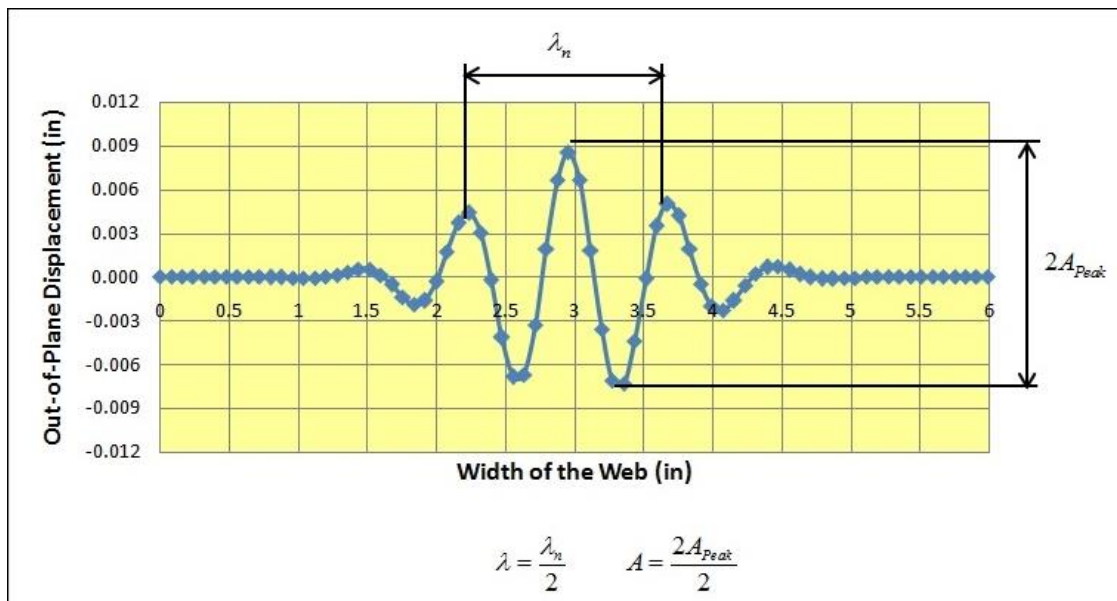


Figure 6-32 - Depicting the Measurement of Wavelength and Amplitude (Abaqus Results)

Strain levels ranging from 0.00116 to 0.00868 were simulated. Results for two strain levels are shown in Figures 6-33 and 6-34.

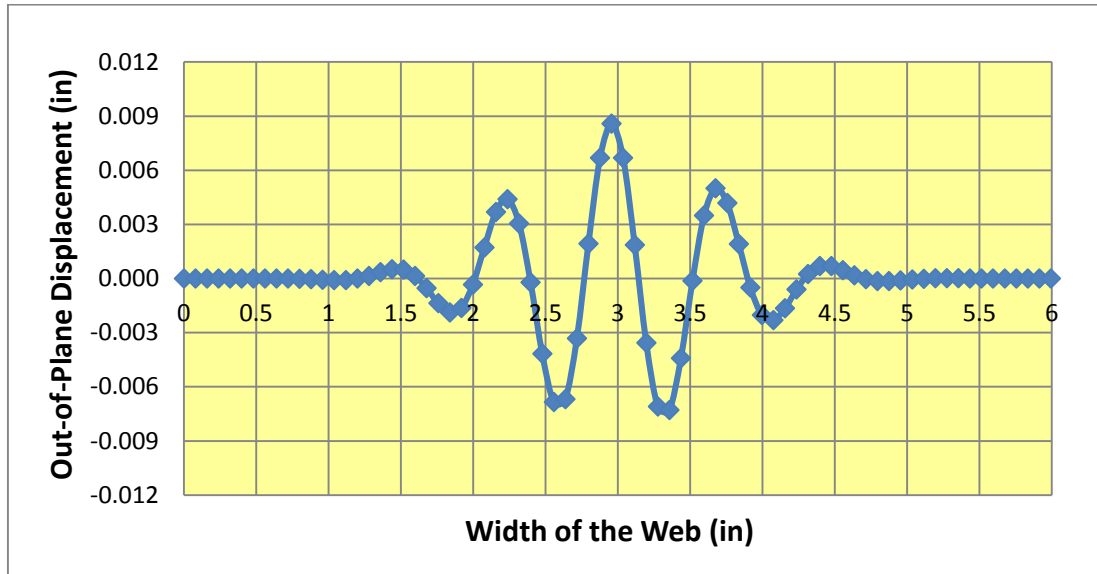


Figure 6-33 - Abaqus Results for the Orthotropic Web at a Strain Level of 0.0034

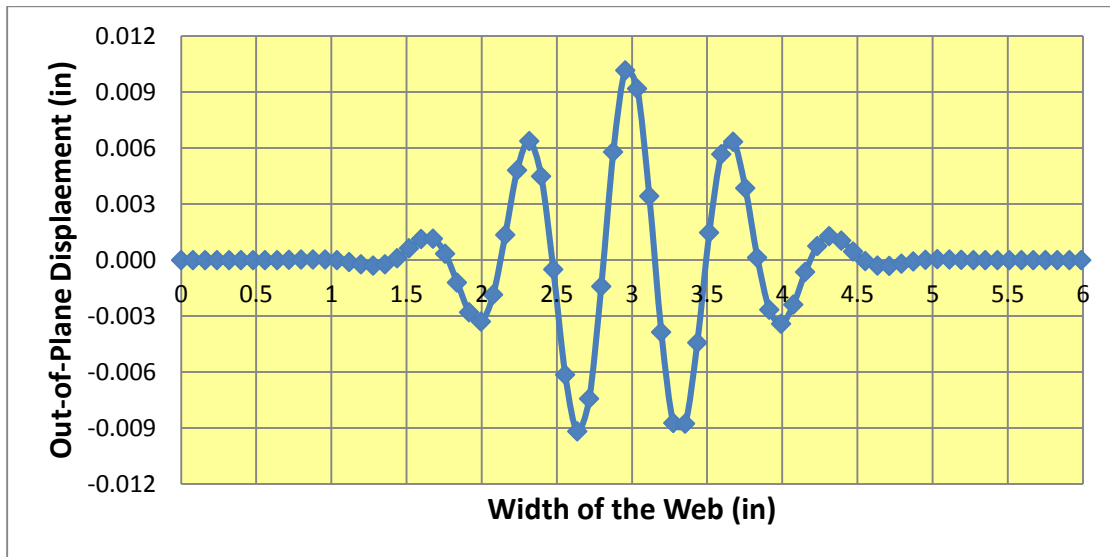


Figure 6-34 - Abaqus Results for the Orthotropic Web at a Strain Level of 0.0063

The contour of the CMD compressive stresses from the Abaqus results is plotted to compare it with the critical compressive stress of orthotropic web.

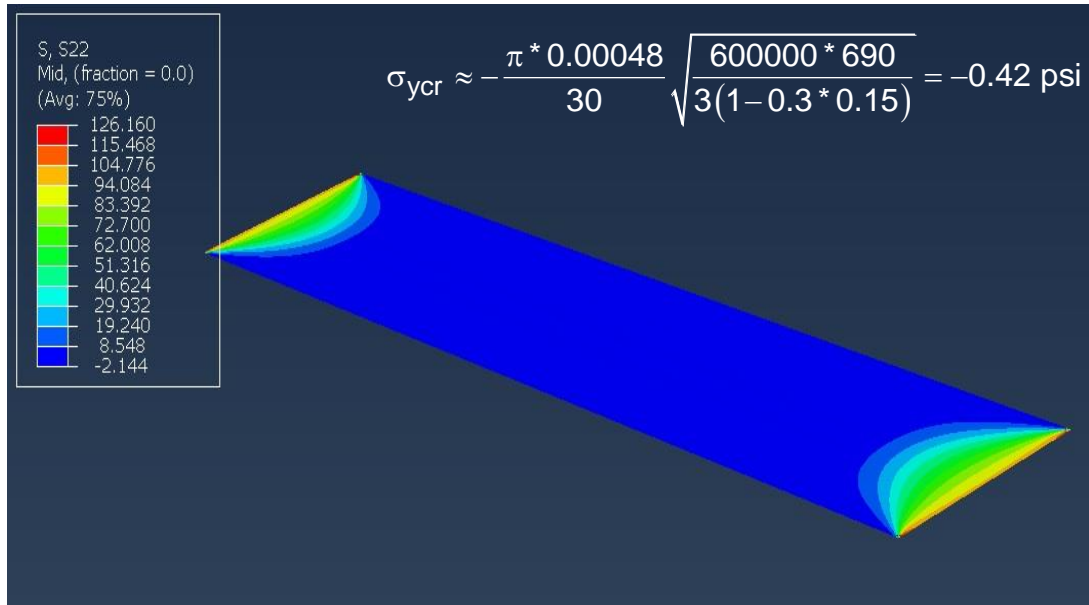


Figure 6-35 - CMD Stresses in the Orthotropic Web (Pseudo Material)

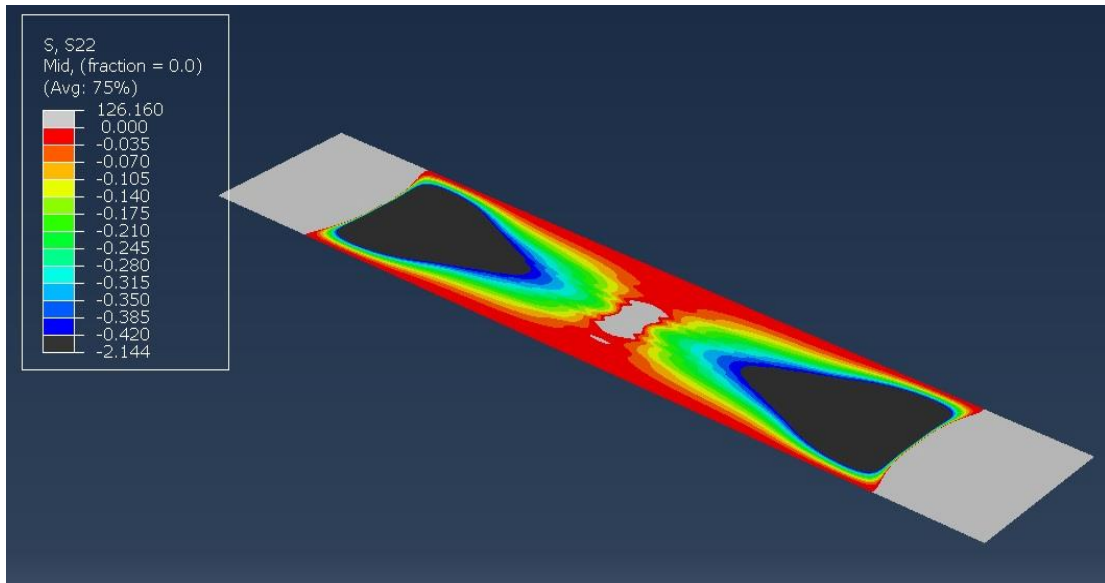


Figure 6-36 - CMD Stresses in the Orthotropic Web with Refined Scale (Pseudo Material)

From Figures 6-35 and 6-36, the CMD compressive stresses in the web at a strain level of 0.0012 are higher than the critical compressive stress of the orthotropic web given by equation (17). Similar to the isotropic web contours for CMD compressive stresses, the orthotropic web have an area of CMD tensile stresses near the clamps and a pocket of CMD compressive stresses away from clamps. These compressive stresses are responsible for the buckling of web.

Tables 6-10 and 6-11 shows the Abaqus results of Wavelength and Amplitude compared with that of theoretical results. Theoretical results for Wavelength and Amplitude are calculated using the equations (18) and (52). Figures 6-35 and 6-36 shows the comparison of Theoretical Wavelength and Amplitude with Abaqus results respectively.

Comparison of Wavelength (in)		
Strain (in/in)	Abaqus	Good (18)
0.0006	-	1.2535
0.0012	1.0396	1.0540
0.0017	0.8795	0.9524
0.0023	0.7994	0.8863
0.0029	0.7593	0.8383
0.0035	0.7193	0.8009
0.0041	0.7191	0.7706
0.0046	0.6791	0.7453
0.0052	0.6789	0.7237
0.0058	0.6788	0.7049
0.0064	0.6388	0.6883
0.0069	0.6387	0.6735
0.0075	0.6386	0.6601
0.0081	0.5985	0.6480
0.0087	0.5984	0.6369

Table 6-10 - Comparison of Abaqus and Theoretical Wavelength on the Orthotropic Web

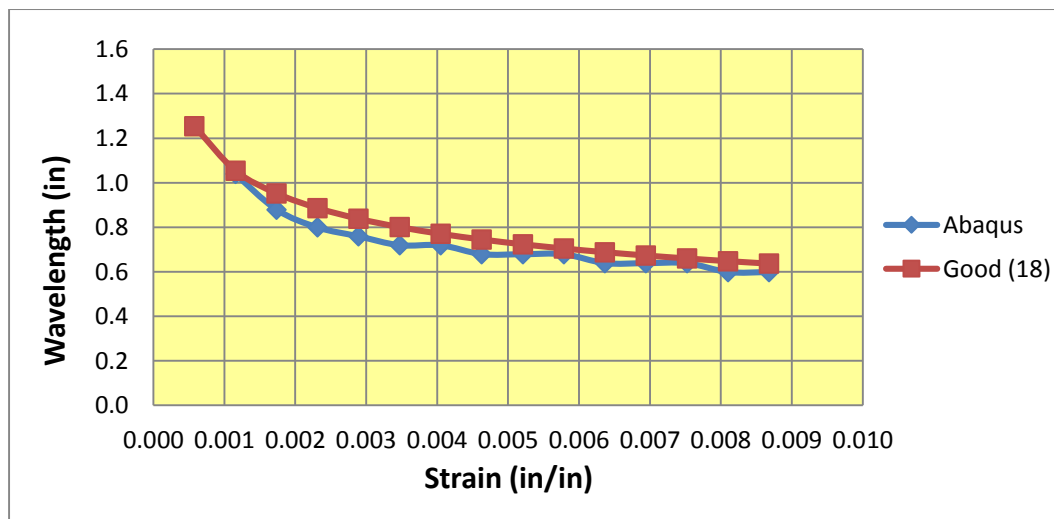


Figure 6-37 - Comparison of Abaqus and Theoretical Wavelength on the Orthotropic Web

Comparison of Amplitude (in)		
Strain (in/in)	Abaqus	Nukala (52)
0.0006	-	0.0053
0.0012	0.0043	0.0063
0.0017	0.0051	0.0069
0.0023	0.0062	0.0074
0.0029	0.0072	0.0079
0.0035	0.0079	0.0082
0.0041	0.0087	0.0086
0.0046	0.0092	0.0088
0.0052	0.0095	0.0091
0.0058	0.0098	0.0093
0.0064	0.0102	0.0096
0.0069	0.0107	0.0098
0.0075	0.0112	0.0100
0.0081	0.0115	0.0102
0.0087	0.0117	0.0103

Table 6-11 - Comparison of Abaqus and Theoretical Amplitude on the Orthotropic Web

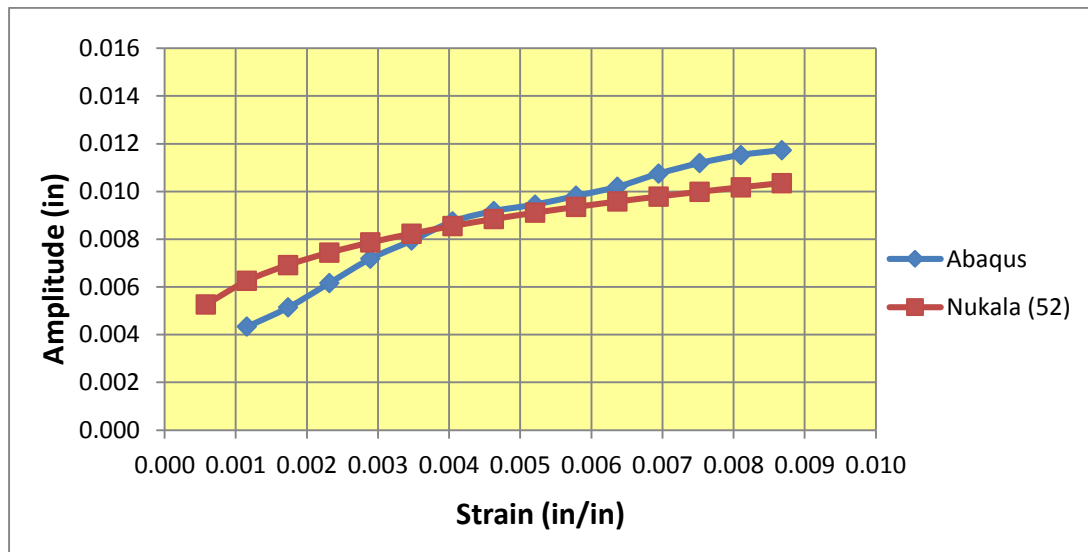


Figure 6-38 - Comparison of Abaqus and Theoretical Amplitude on the Orthotropic Web

The results shown in Figure 6-35 show that the equation (18) predicts the buckled wavelength of an orthotropic web very well. The results shown in Figure 6-36 show good agreement between equation (52) and the Abaqus results. Again, there is disagreement at low strain levels where the CMD stresses were insufficient to buckle the web.

CHAPER VII

CONCLUSIONS AND FUTURE WORK

Conclusions

Experiments and Abaqus simulations were conducted to validate the expressions for amplitude and wavelength of troughs formed in both isotropic and orthotropic webs. The conclusions of this study are as follows:

- 1) The equations of troughs wavelength for isotropic and orthotropic webs ((**8**), (**18**) and (**38**)) compare well with experiment and Abaqus simulations as demonstrated in Figures 6-14, 6-30 and 6-35. Since, the amplitude equations derived from theory of inextensibility assumptions depend on either half wave number, n or wavelength, $\lambda = \frac{2b}{n}$ this is an important finding.
- 2) The equations of trough amplitude for isotropic and orthotropic webs ((**44**) and (**52**)) developed based on the assumption of inextensibility compare well with finite element simulations as shown in Figures 6-15 and 6-36. These equations also envelop experiment results over some domain of strain as shown in Figures 6-15 and 6-31. As such it is concluded that these equations do have value for process engineers who are concerned with trough amplitude effects on process.
- 3) In an orthotropic web, the Abaqus simulations show no signs of buckling as the critical compressive stress is greater than the CMD compressive stresses. However, the signs

of buckling was witnessed while conducting the experiments. It is believed that the web buckled because of non-uniformity of the web thickness as shown in Figure 6-28.

- 4) When the same experiment was repeated on different samples of orthotropic web, the profile of troughs shown in Figures 6-21, 6-22 and 6-23 were not as consistent as they were for an isotropic web shown in Figures 6-4, 6-5 and 6-6. It is believed that this phenomenon is a result of the variation in thickness across the web.

Future Study

- 1) Experiments exhibited large trough amplitudes at low strain levels. This behavior was also witnessed by Zheng[10]. This behavior should be explored in simulations by simulating the clamping process used in tests. It is hypothesized that the clamping process may be inducing compressive CMD stress as the clamp pressure increases. These stresses may buckle the web prior to stretching.
- 2) The amplitude equations ((44) and (52)) are monotonically increasing with strain. Zheng[10] demonstrates that with increased high strain levels that the trough amplitude will diminish and return to zero (hence the troughs vanish) by simulation and by experiments. This infers that high web tensions/strains will act to diminish the out-of-plane deformations (large deformation theory). It would be included in amplitude expressions. This may include an added complexity of material nonlinearity.
- 3) The effects of material non-uniformity on instability in webs would be a valuable study. The orthotropic web studied in the laboratory in this investigation was assumed to have constant thickness and material properties when buckling simulations were performed in Abaqus. While buckling was observed in the laboratory no buckling was observed in the simulations. It was hypothesized that if the web thickness and material properties were known spatially throughout the web coupons tested, and those variations were input to the simulations, that buckling would have also resulted in the simulations. To prove this

hypothesis would require that non-destructive methods be developed to assess the thickness and property variation in a web coupon prior to buckling tests. Although non-destructive means of assessing thickness variation exist future investigators would need to develop means to assess the spatial property variation in the orthotropic Young's moduli and Poisson's ratio.

REFERENCES

- 1) Beisel, J.A. and Good, J.K., *The Instability of Webs in Transport*, ASME Journal of Applied Mechanics, V78, 011001-1-7, January 2011.
- 2) E. Cerda, L. Mahadevan, *Wrinkling of an Elastic Sheet Under Tension*, Nature Publishing Group, 2002, Vol. 419.
- 3) E. Cerda, L. Mahadevan, *Geometry and Physics of Wrinkling*, UK: The American Physical Society, 2003.
- 4) S.P. Timoshenko, J. M. Gere., *Theory of Elastic Stability*, Second Edition, New York, McGrawHill, 1961, p. 348.
- 5) Good, J.K. and Beisel, J.A., “*Calculations Related to Web Buckling Resulting from Roller Misalignment*”, TAPPI Journal, V5, N12, p. 9-16.
- 6) J.K. Good, J.A. Beisel, H. Yurtcu., *Instability of Webs: The Prediction of Troughs and Wrinkles*, Stillwater, Oxford, 2009, Vol. 1.
- 7) S.G. Lekhnitskii., *Anisotropic Plates*, Second Edition, New York, Gordon and Breach, 1968.
- 8) Good, J. K., *Proceedings of the Web Handling Research Center Industrial Advisory Board Meeting*”, November, 2015, Tab 4.
- 9) Vishal Nayyar, K. Ravi-Chandar and Rui Huang., *Stretch-induced stress patterns and wrinkles in hyperelastic thin sheets*, Elsevier International Journal of Solids and Structures, 2011.

- 10) Zheng, L., *Wrinkling of Dielectric Elastomer Membranes*, Ph. D. Thesis, California Institute of technology, 2009, Fig 5.3, page 97.

APPENDICES

The profile of troughs formed on an isotropic web at various strains that were not presented in results section are shown in the plots below.

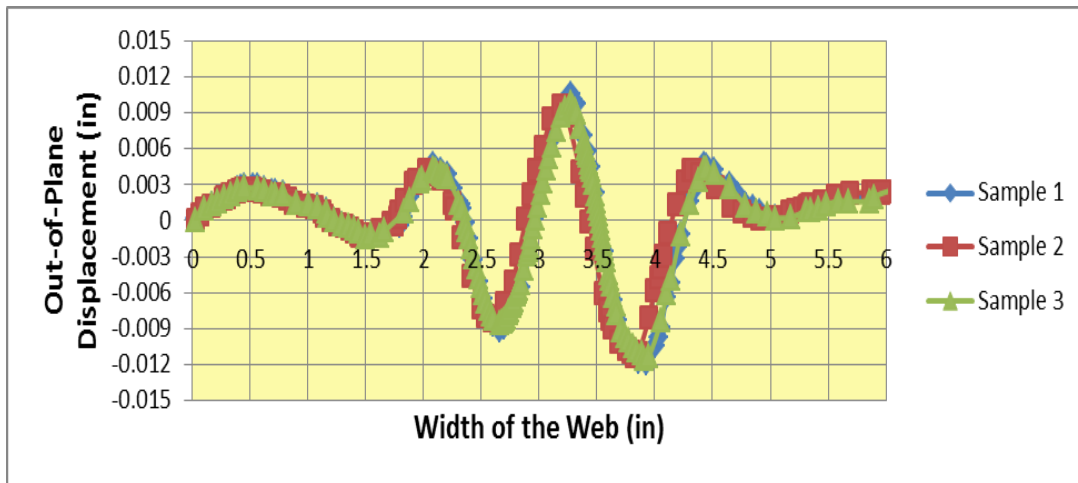


Figure A-1 – Repeatability Test for Troughs in the Isotropic Web at a Strain Level of 0.0012

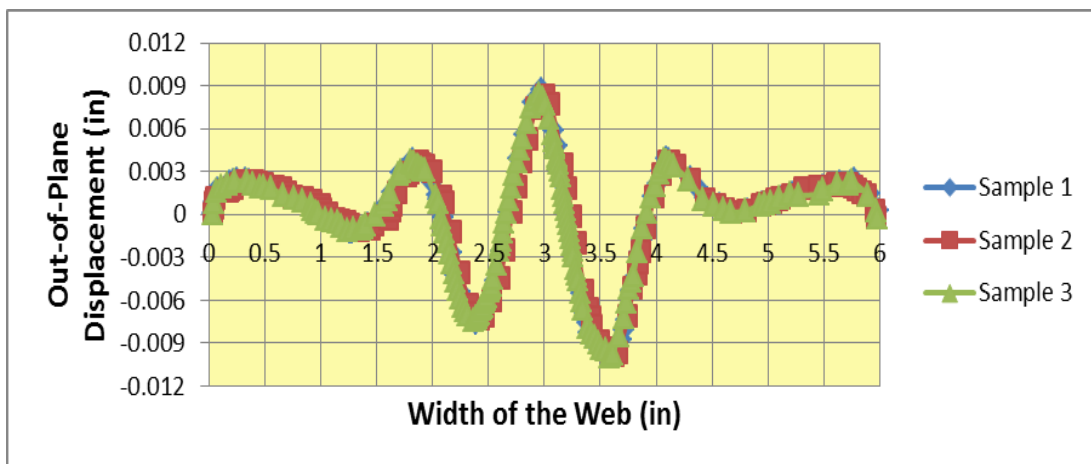


Figure A-2 - Repeatability Test for Troughs in the Isotropic Web at a Strain Level of 0.0017

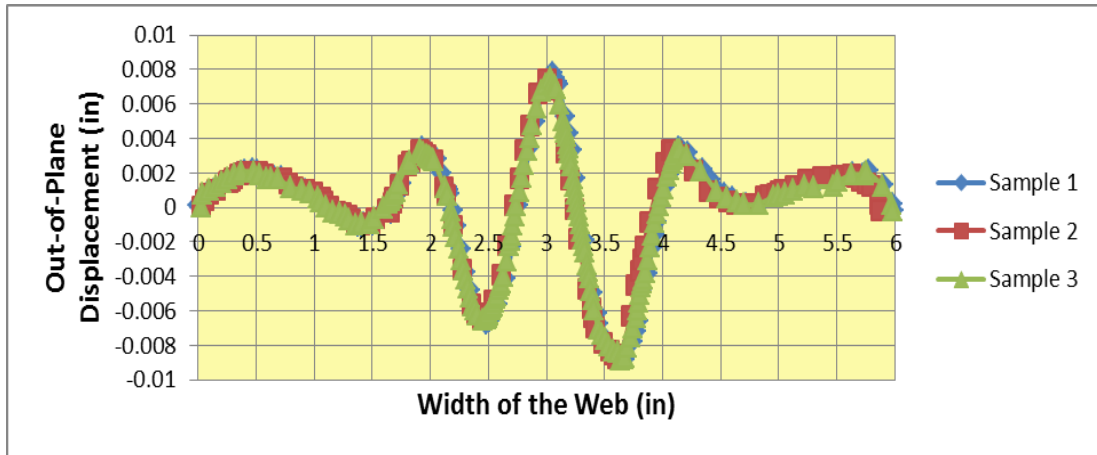


Figure A-3 - Repeatability Test for Troughs in the Isotropic Web at a Strain Level of 0.0023

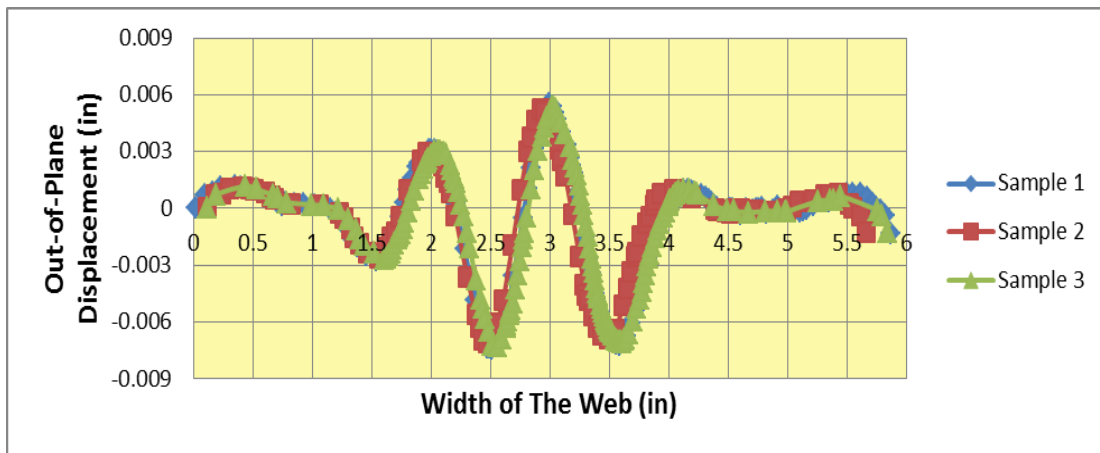


Figure A-4 - Repeatability Test for Troughs in the Isotropic Web at a Strain Level of 0.0035

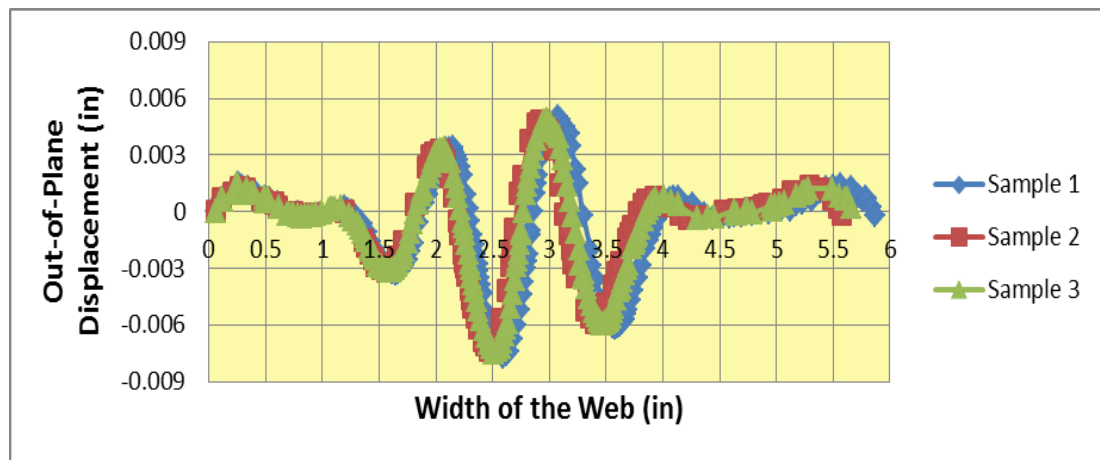


Figure A-5 - Repeatability Test for Troughs in the Isotropic Web at a Strain Level of 0.0041

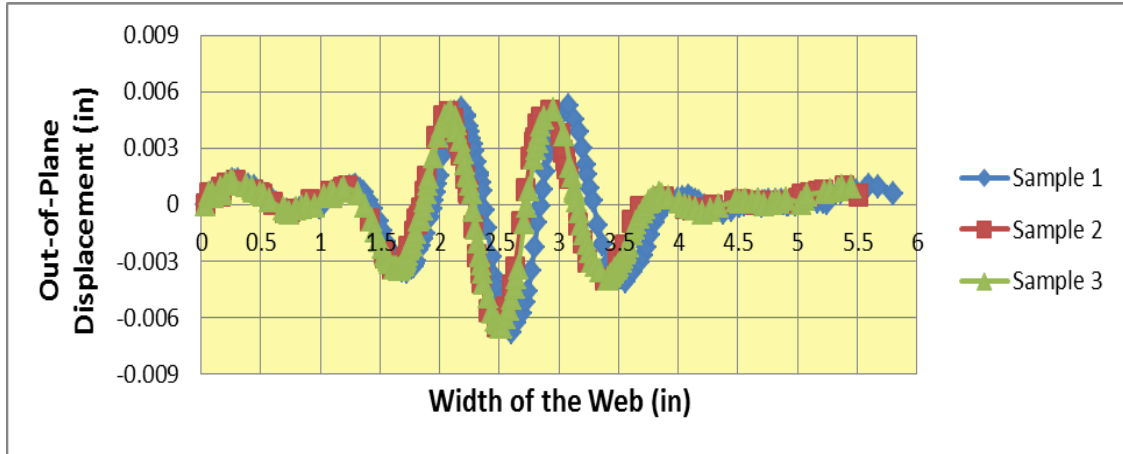


Figure A-6 - Repeatability Test for Troughs in the Isotropic Web at a Strain Level of 0.0052

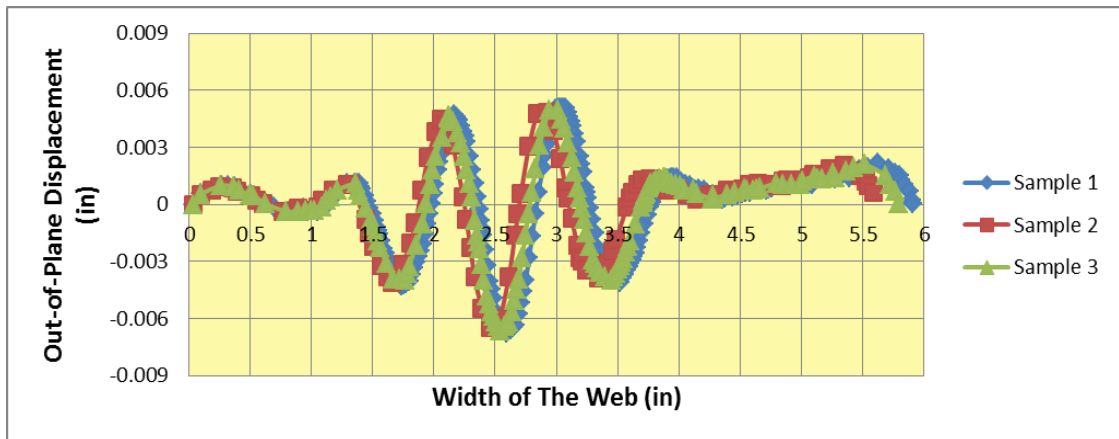


Figure A-7 - Repeatability Test for Troughs in the Isotropic Web at a Strain Level of 0.0058

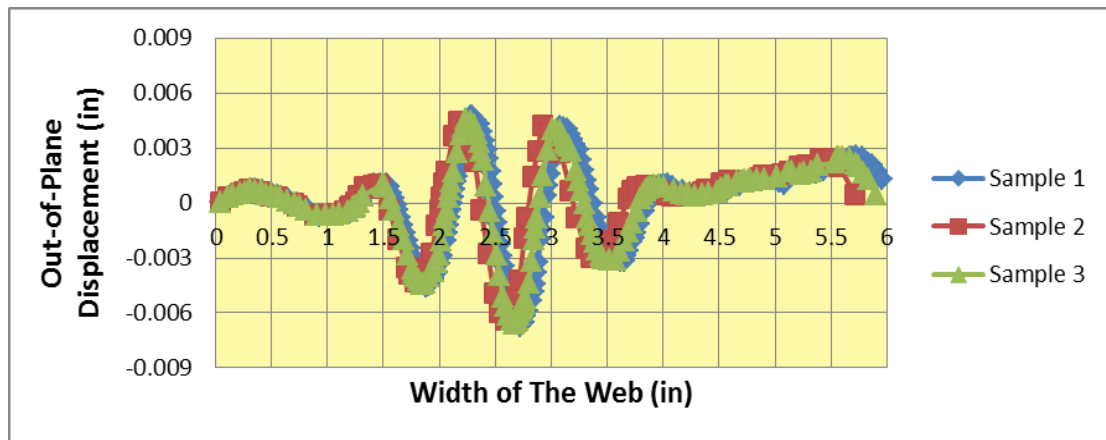


Figure A-8 - Repeatability Test for Troughs in the Isotropic Web at a Strain Level of 0.0064

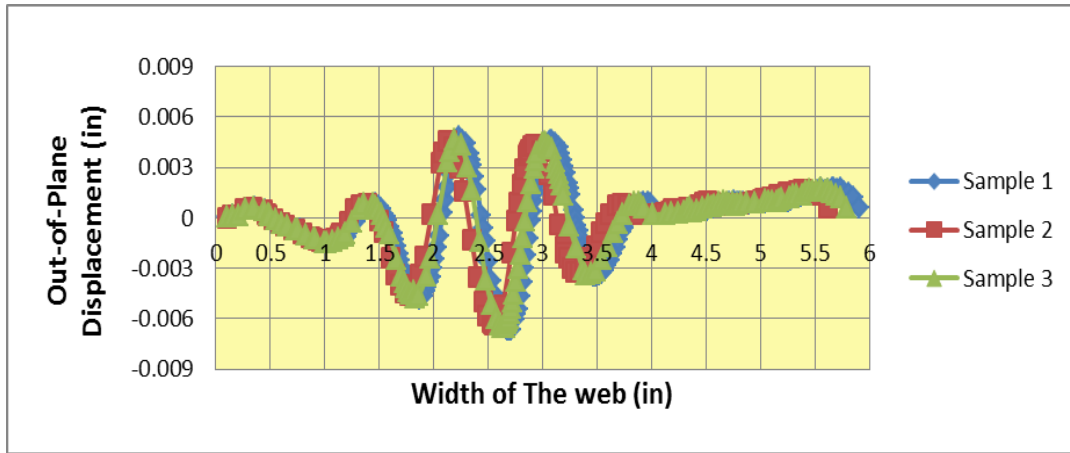


Figure A-9 - Repeatability Test for Troughs in the Isotropic Web at a Strain Level of 0.0069

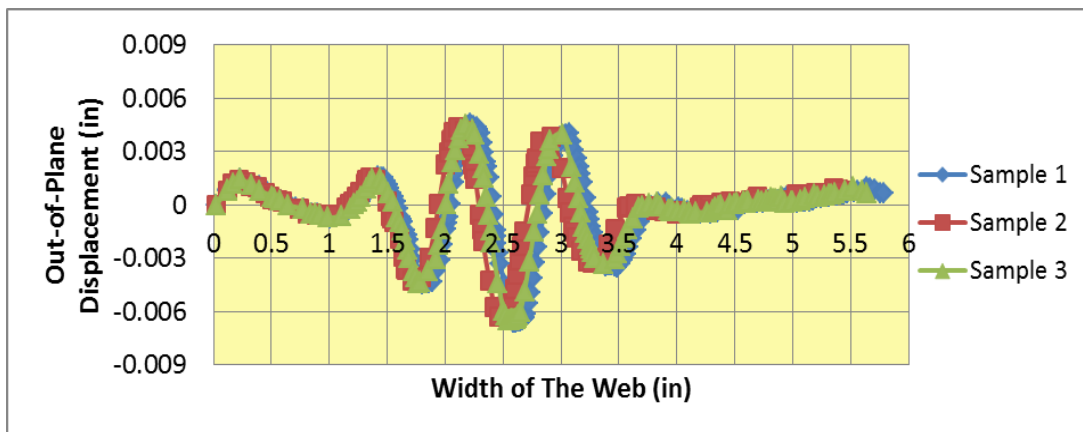


Figure A-10 - Repeatability Test for Troughs in the Isotropic Web at a Strain Level of 0.007

The Abaqus results of profile of troughs formed on an isotropic web are plotted below,

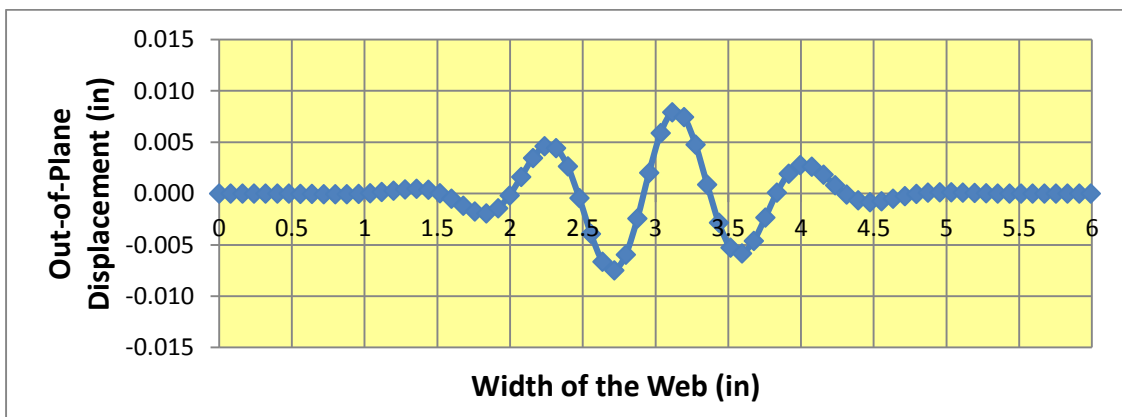


Figure A-11 - Abaqus Results of Troughs on Isotropic Web at a Strain Level of 0.0035

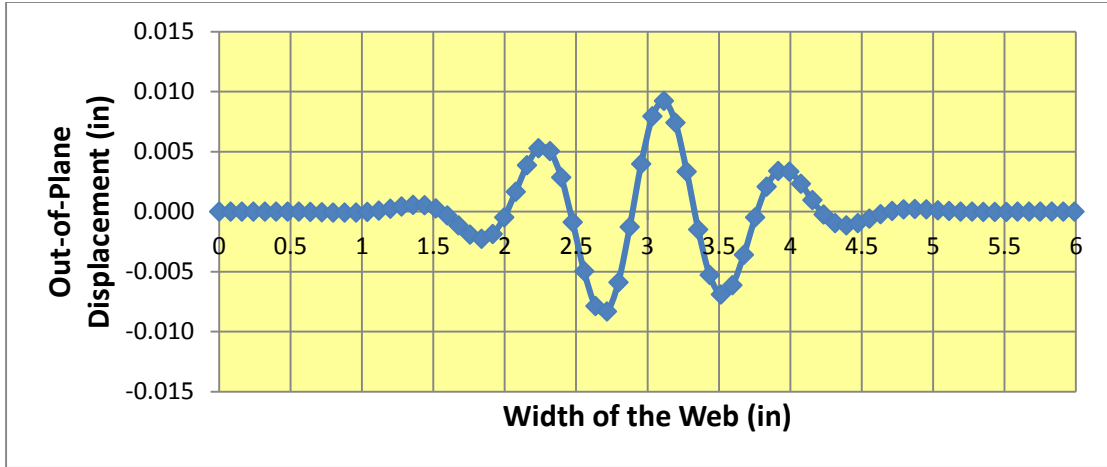


Figure A-12 - Abaqus Results of Troughs on Isotropic Web at a Strain Level of 0.0041

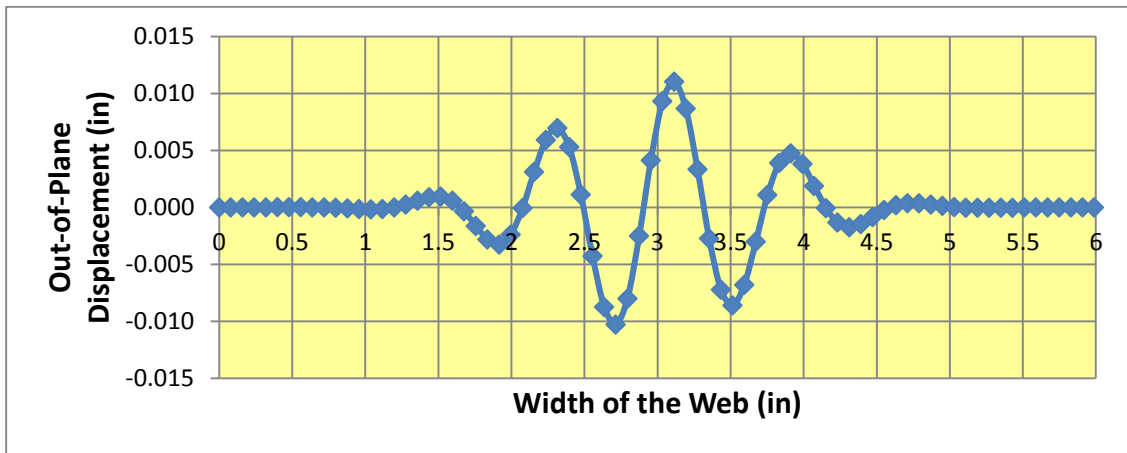


Figure A-13 - Abaqus Results of Troughs on Isotropic Web at a Strain Level of 0.0052

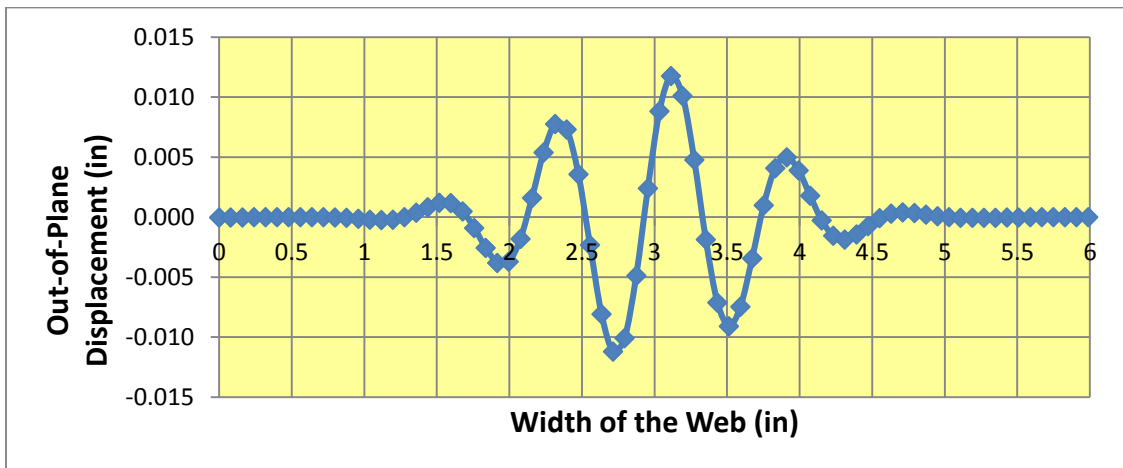


Figure A-14 - Abaqus Results of Troughs on Isotropic Web at a Strain Level of 0.0058

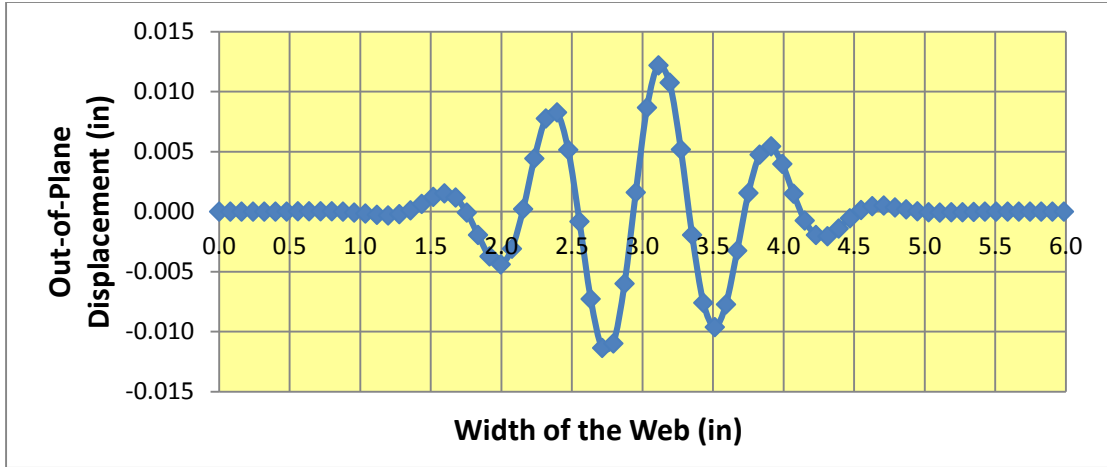


Figure A-15 - Abaqus Results of Troughs on Isotropic Web at a Strain Level of 0.0064

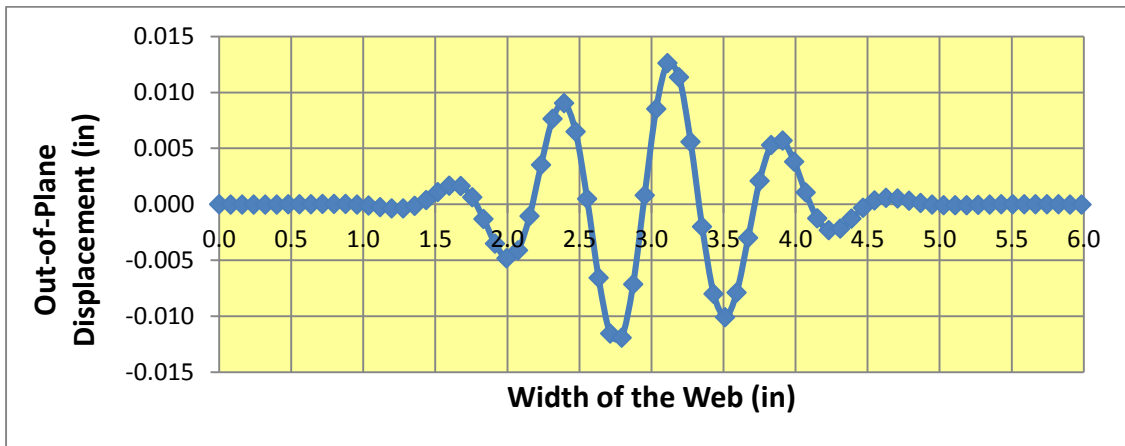


Figure A-16 - Abaqus Results of Troughs on Isotropic Web at a Strain Level of 0.0069

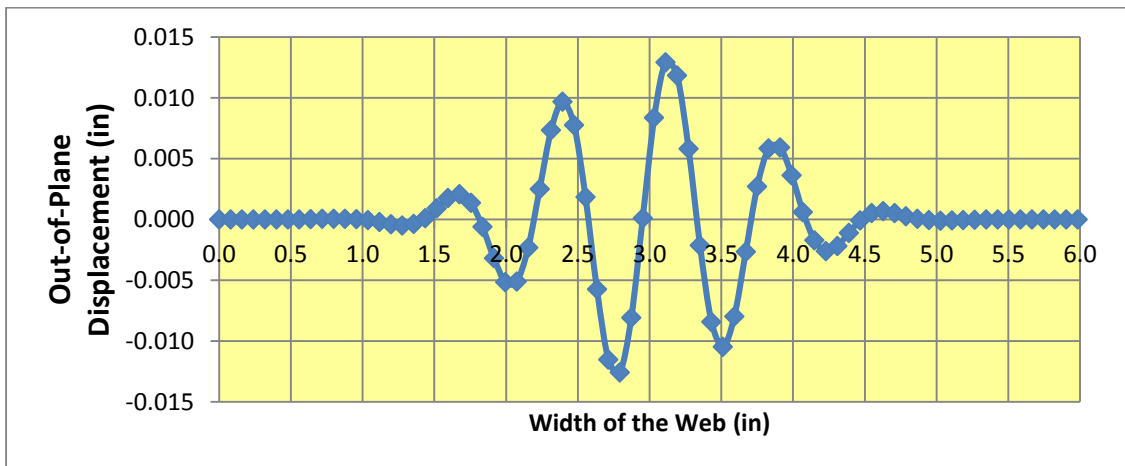


Figure A-17 - Abaqus Results of Troughs on Isotropic Web at a Strain Level of 0.0075

The profile of troughs formed on an orthotropic web at various strains that were skipped in results section are shown in the plots below.

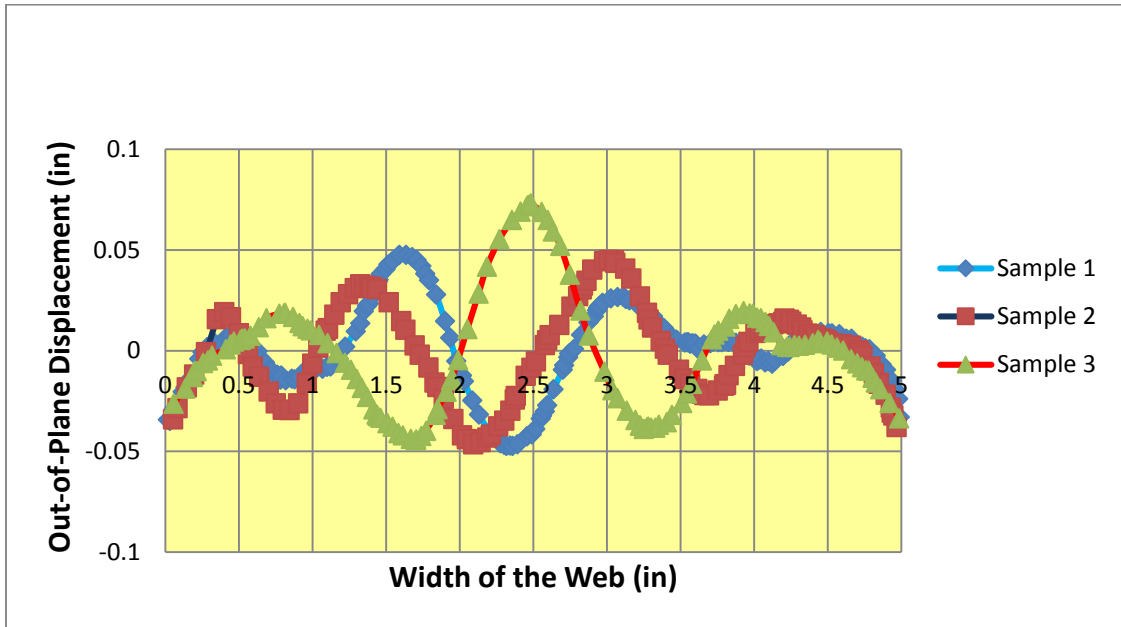


Figure A-18 – Repeatability Tests for Troughs in Orthotropic Web at a Strain Level 0.009

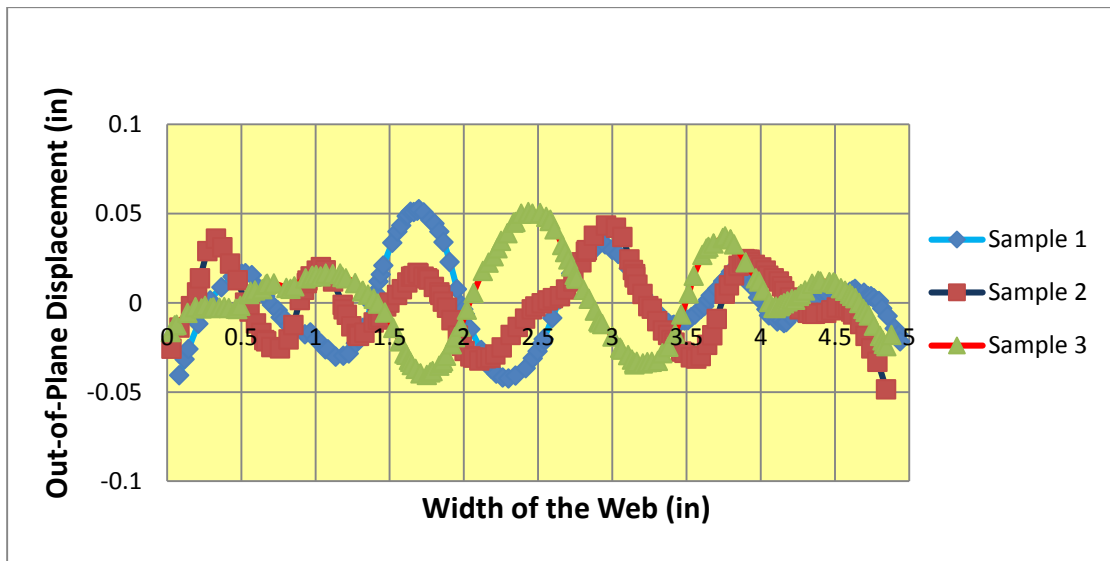


Figure A-19 - Repeatability Tests for Troughs in Orthotropic Web at a Strain Level 0.015

VITA

VINDHYA NUKALA

Candidate for the Degree of

Master of Science

Thesis: PREDICTION OF AMPLITUDE OF STRETCH INDUCED TROUGHS

Major Field: Mechanical and Aerospace Engineering

Biographical:

Education:

Completed the requirements for the Master of Science in Mechanical and Aerospace Engineering at Oklahoma State University, Stillwater, Oklahoma in July, 2016.

Completed the requirements for the Bachelors of Technology in Mechanical Engineering at Jawaharlal Nehru Technological University, Hyderabad, Telangana, India in 2013.